Lithos 380–381 (2021) 105893

Contents lists available at ScienceDirect

Lithos

journal homepage: www.elsevier.com/locate/lithos

Research Article

Origin of geochemically heterogeneous mid-ocean ridge basalts from the Macquarie Ridge Complex, SW Pacific

Qiang Jiang [a,b,*], Renaud E. Merle [c,d], Fred Jourdan [a,b], Hugo K.H. Olierook [b,e,f], Massimo Chiaradia [g], Katy A. Evans [b], Xuan-Ce Wang [h,i,j], Chris E. Conway [k], Helen C. Bostock [j,l], Richard J. Wysoczanski [l]

[a] Western Australian Argon Isotope Facility & John de Laeter Centre, Curtin University, Perth, WA 6845, Australia
[b] School of Earth and Planetary Sciences, Curtin University, Perth, WA 6845, Australia
[c] Department of Geosciences, Swedish Museum of Natural History, S-104 05 Stockholm, Sweden
[d] Department of Earth Sciences, Natural Resources and Sustainable Development, Uppsala University, Villavägen 16, 75236 Uppsala, Sweden
[e] Timescales of Mineral Systems, Centre for Exploration Targeting – Curtin Node, School of Earth and Planetary Sciences, Curtin University, Perth, WA 6845, Australia
[f] John de Laeter Centre, Curtin University, Perth, WA 6845, Australia
[g] Department of Earth Sciences, University of Geneva, Rue des Maraîchers 13, 1205 Geneva, Switzerland
[h] Research Centre for Earth System Science, Yunnan Key Laboratory of Earth System Science, Yunnan University, Kunming 650500, China
[i] School of Earth Science and Resources, Chang'an University, Xi'an 710054, China
[j] School of Earth and Environmental Sciences, The University of Queensland, Brisbane, QLD 4072, Australia
[k] Institute of Earthquake and Volcano Geology, Geological Survey of Japan, AIST, Central 7, 1-1-1, Higashi, Tsukuba, Ibaraki 305-8567, Japan
[l] National Institute of Water and Atmospheric Research, Private Bag 14-901, Wellington 6241, New Zealand

ARTICLE INFO

Article history:
Received 23 August 2020
Received in revised form 15 November 2020
Accepted 15 November 2020
Available online 24 November 2020

Keywords:
Balleny plume
HIMU
Macquarie Island
Mantle metasomatism
Pyroxenite
Zealandia

ABSTRACT

The Macquarie Ridge Complex (MRC), located at the Australian–Pacific plate boundary south of New Zealand, is a rugged bathymetric ridge comprising a series of submarine seamounts and Macquarie Island, the only subaerial portion of the complex. Mid-ocean ridge basalts (MORBs) from Macquarie Island show various enrichments in incompatible elements with compositions ranging from typical normal MORB to enriched MORB. However, these basalts have isotopic compositions trending towards a high μ-like ($\mu = {}^{238}U/{}^{204}Pb$; HIMU) mantle component, which is unusual for MORB-type rocks. The origin of this mantle signature is not understood, and it is unclear whether this isotopic signature is characteristic of the entire MRC or unique to Macquarie Island. Here we report new major and trace element abundances, and Sr, Nd, and Pb isotopes for samples from the MRC seamounts and from new sampling sites on Macquarie Island. The geochemical and isotopic data show that the entire MRC comprises normal to enriched MORB. Mixing modelling indicates that the heterogeneous isotopic signatures of the MRC basalts are not derived from contamination of the nearby Balleny mantle plume but have affinities with that of the Cenozoic Zealandia intraplate HIMU-like basalts. We propose that the heterogeneous geochemical signatures of the MRC basalts are derived from amphibole-bearing garnet pyroxenite veins, which is supported by the rare earth element partial melting modelling and strong correlations between Nd and Pb isotopic ratios vs La/Sm. We posit that the pyroxenite veins were generated in the oceanic lithospheric mantle, which was metasomatised by hydrous and carbonatitic fluids/melts derived either from delaminated, metasomatised Zealandia subcontinental lithosphere mantle, or from subducted material in the asthenosphere. The subducted material could be derived from ancient and/or recent subduction along the former east Gondwana margin.

1. Introduction

Oceanic basalts, including ocean island basalts (OIBs) and mid-oceanic ridge basalts (MORBs), provide a unique window to understand the chemical compositions of Earth's mantle. Mid-ocean ridge basalts are the most voluminous and widely distributed magmatic products on Earth (Saunders et al., 1988). Although it is believed that the mantle source of MORB is depleted by melt extraction and homogenized by convective stirring (e.g., Hofmann, 1988), an increasing number of studies have shown that the mantle sources of MORB could be heterogeneous (e.g., Borghini et al., 2020; Hofmann, 2003). While mantle plume contaminations have often been invoked to explain the source heterogeneity of MORB at a local scale (e.g., Schilling et al., 1994), other mechanisms may also have played a role, particularly for

* Corresponding author at: Western Australian Argon Isotope Facility, School of Earth and Planetary Sciences, Curtin University, Perth, WA 6845, Australia.
E-mail address: qiang.jiang1@postgrad.curtin.edu.au (Q. Jiang).

https://doi.org/10.1016/j.lithos.2020.105893
0024-4937/

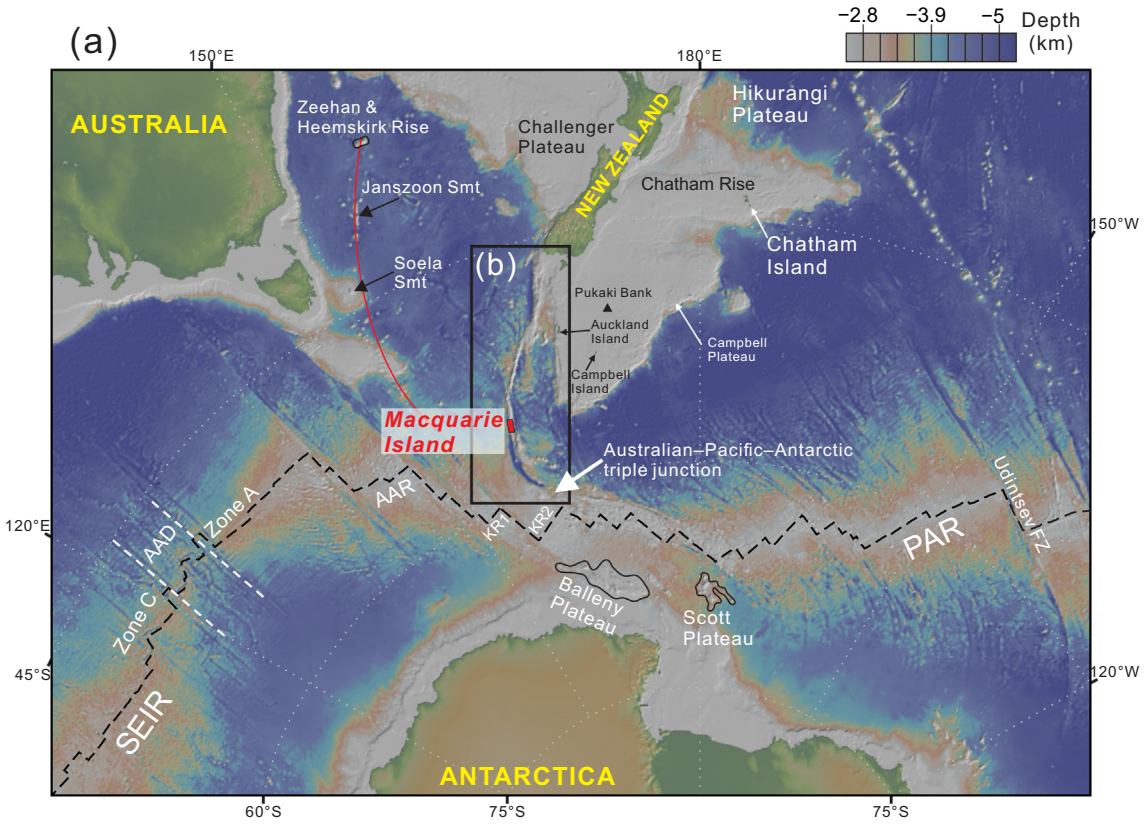
(a)
−2.8
−3.9
−5
Depth (km)
150°E
180°E
150°W
120°W
120°E
45°S
60°S
75°S
75°S
AUSTRALIA
ANTARCTICA
Zeehan & Heemskirk Rise
Challenger Plateau
NEW ZEALAND
Hikurangi Plateau
Janszoon Smt
Chatham Rise
Chatham Island
Soela Smt
(b)
Pukaki Bank
Auckland Island
Campbell Plateau
Campbell Island
Macquarie Island
Australian–Pacific–Antarctic triple junction
AAR
KR1
KR2
PAR
Udintsev FZ
AAD
Zone A
Zone C
SEIR
Balleny Plateau
Scott Plateau

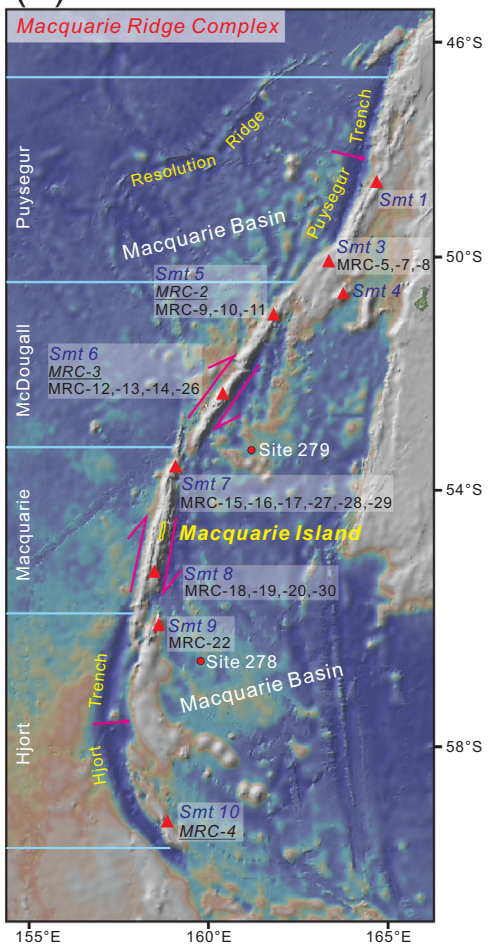
(b)
Macquarie Ridge Complex
46°S
50°S
54°S
58°S
155°E
160°E
165°E
Puysegur
McDougall
Macquarie
Hjort
Resolution Ridge
Puysegur Trench
Trench
Hjort
Macquarie Basin
Macquarie Basin
Smt 1
Smt 3
MRC-5,-7,-8
Smt 5
MRC-2
MRC-9,-10,-11
Smt 4
Smt 6
MRC-3
MRC-12,-13,-14,-26
Site 279
Smt 7
MRC-15,-16,-17,-27,-28,-29
Macquarie Island
Smt 8
MRC-18,-19,-20,-30
Smt 9
MRC-22
Site 278
Smt 10
MRC-4

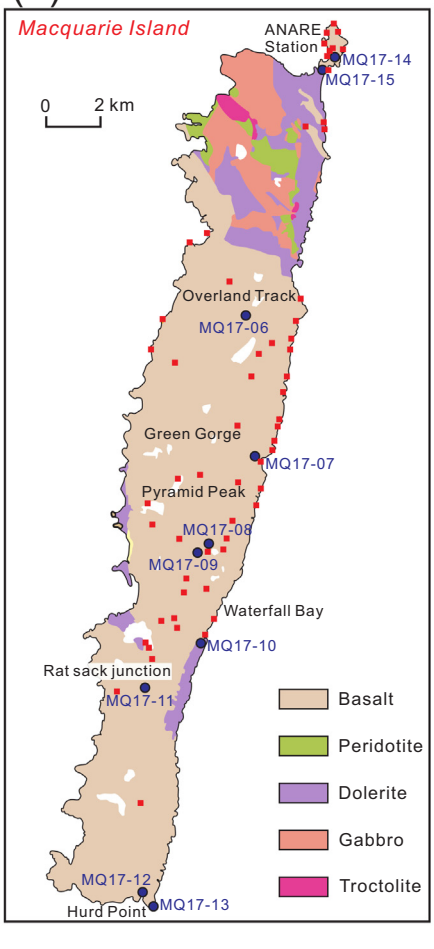
(c)
Macquarie Island
ANARE Station
MQ17-14
MQ17-15
0
2 km
Overland Track
MQ17-06
Green Gorge
MQ17-07
Pyramid Peak
MQ17-08
MQ17-09
Waterfall Bay
MQ17-10
Rat sack junction
MQ17-11
MQ17-12
Hurd Point
MQ17-13
Basalt
Peridotite
Dolerite
Gabbro
Troctolite

large-scale heterogeneities, such as recycling of oceanic crust and sediment (Rehkämper and Hofmann, 1997), lower continental crust (Kamenetsky et al., 2001), or delaminated subcontinental lithospheric mantle (SCLM; Goldstein et al., 2008).

On the basis of geochemical analyses of samples from Macquarie Island, previous studies have identified a domain of heterogeneous MORB in the southwestern Pacific Ocean (Fig. 1). The Macquarie Island basalts display a large range of incompatible element enrichments varying from typical normal MORB (N-MORB) to enriched MORB (E-MORB; Kamenetsky et al., 2000). These basalts have incompatible element patterns showing similarities with HIMU (high $\mu = {}^{206}Pb/{}^{238}U$) OIBs and isotopic signatures trending towards a HIMU-like ($^{206}Pb/^{204}Pb > 19.5$; Stracke et al., 2005) mantle component (Kamenetsky et al., 2000; Kamenetsky and Maas, 2002). Such mantle signatures are more commonly associated with OIBs (e.g., Chaffey et al., 1989), but are rare at mid-ocean ridges. The origin of the distinct incompatible element patterns and heterogeneous isotopic signatures of the Macquarie Island MORB is, however, not clearly understood. It has been speculated that this heterogeneous mantle component was either derived from the Balleny mantle plume, based on the adjacent position of the hotspot track to the Macquarie Ridge (Fig. 1a), or that it is a broader regional signature in the shallow mantle that is characteristic of the SW Pacific Ocean (Finn et al., 2005; Kamenetsky et al., 2000; Lanyon, 1994; Pyle et al., 1995).

The ~37 km-long Macquarie Island is the only emerged portion of the ~1600 km-long Macquarie Ridge Complex (MRC), a NE–SW trending fossil mid-ocean ridge located along the Australian–Pacific plate boundary south of New Zealand (Conway et al., 2012; Massell et al., 2000; Mosher and Symons, 2008). The small size of Macquarie Island relative to the entire MRC makes any extrapolation along the ridge difficult, such that it remains unclear whether the heterogeneous mantle signature present at Macquarie Island is: (i) evidence of source heterogeneity intrinsic to the upper mantle but restricted to the proximity of the island (Kamenetsky et al., 2000; Kamenetsky and Maas, 2002); (ii) symptomatic of the entire MRC region; or (iii) a result of direct enrichment of asthenosphere derived from the Balleny mantle plume (Lanyon, 1994; Lanyon et al., 1993; Pyle et al., 1995).

In this paper, we report a new data set of major elements, trace elements and Sr–Nd–Pb isotopic ratios of basalts collected during a new sampling campaign on Macquarie Island, and previously collected dredged samples from the ~1600 km long, submarine portion of the MRC. Using these new data, we investigate the mantle source characteristics of the MORB of the ~1600 km-long MRC and use the results to develop a new model for the origin of distinctive isotopic signature and source heterogeneity of mid-ocean ridge basalts in this part of the Pacific Ocean.

2. Geological background

2.1. Macquarie Ridge Complex

The MRC, which is located to the west of the microcontinent Zealandia, extends from the southern tip of New Zealand to the Australian–Pacific–Antarctic triple junction (Fig. 1a; Massell et al., 2000). It can be divided into four segments separated by discontinuities and changes in orientation. From south to north these are the Hjort, Macquarie, McDougall and Puysegur segments (Fig. 1b; Massell et al., 2000). The MRC formed during relatively rapid plate motions between the Australian and Pacific plates in three distinct phases. (1) At ~40 Ma, seafloor spreading initiated and oceanic crust was generated in the proto-Macquarie spreading centre. (2) From 30 Ma, the Macquarie spreading ridge gradually became oblique to the Pacific–Australian plate boundary due to changes in relative plate motion between the two plates (Massell et al., 2000). The spreading ridge segments shortened, and curved fracture zones formed to accommodate the changes in spreading direction (Mosher and Symons, 2008). (3) By ~6 Ma, the relative motions of the Pacific and Australian plates became so oblique that spreading and related magmatism ceased (Meckel, 2003). The MRC has since transitioned from mid-ocean ridge spreading to strike-slip motion in the center (McDougall and Macquarie segments) and incipient oceanic–oceanic subduction in the southern (Hjort) and northern (Puysegur) segments to accommodate the convergence between the Australian and Pacific plates (Meckel, 2003).

The multi-stage plate–plate interactions left a record of magmatism represented by mafic extrusive and intrusive rocks on the island and seamounts, and exhumation of the lithospheric mantle (peridotites) that are now exposed on the northern part of Macquarie Island. The age of the seamount basalts has not been investigated so far but will form part of a subsequent contribution. The basalts on the Macquarie Ridge were formed during the final stages of seafloor spreading of the proto-Macquarie spreading center when spreading segments were still able to sustain active magmatism (Mosher and Symons, 2008; Wertz, 2003).

Seven of the eleven seamounts on the MRC have been sampled during a RV *Tangaroa* voyage (TAN0803) in 2008 (Fig. 1b; Conway et al., 2012). The vast majority of dredged volcanic rocks are alkaline to subalkaline basalts and preliminary major elemental geochemistry analyses indicate that they are enriched MORB (Conway et al., 2012).

2.2. Macquarie Island

Macquarie Island is a ~ 37 km long and ~ 3–5 km wide elongated island on the Macquarie Ridge formed at ~11 Ma (Duncan and Varne, 1988). It is the only portion of the ridge that is above sea level uplifted by compressive stresses. Lithospheric mantle and oceanic lower crustal lithologies, including peridotites, sheeted dolerite dykes, gabbros and troctolites, occur in the northern quarter of the island whereas the central and southern parts of the island are dominated by oceanic upper crustal assemblages including basaltic pillow lavas and massive to tabular basaltic lavas (Fig. 1c; Dijkstra et al., 2010; Varne et al., 2000).

The chemical compositions of Macquarie Island basaltic glasses have been previously investigated (Kamenetsky et al., 2000; Kamenetsky and Maas, 2002). Most of the analyzed samples are subalkaline basalts (tholeiitic) with a few alkali basalts, and show a range of enrichments in incompatible elements, with characteristics that vary from N-MORB to E-MORB. Isotopic data indicate that the Macquarie Island basalts show great affinity with Pacific MORB, but they have more radiogenic Pb isotopic ratios trending towards HIMU OIBs (Kamenetsky et al., 2000; Kamenetsky and Maas, 2002). The heterogeneous geochemical and isotopic characteristics of the Macquarie Island glasses were proposed to be produced by fractional 'dynamic' melting of a spinel peridotite source, which is isotopically heterogeneous at the grain scale (Husen et al., 2016; Kamenetsky et al., 2000; Kamenetsky and Maas, 2002).

Fig. 1. (a) Bathymetric map of the SW Pacific region showing the location of the Macquarie Ridge Complex. The red line indicates the path of Balleny hotspot track (Lanyon et al., 1993). AAD—Australian–Antarctic Discordance, AAR—Australian–Antarctic Ridge, FZ—Fracture Zone, PAR—Pacific–Antarctic Ridge, SEIR—Southeast Indian Ridge, Smt—Seamount. (b) Bathymetric map of the Macquarie Ridge Complex showing the locations of the seamounts and dredge samples used in this study. Samples MRC-2, –3, –4 (underlined) were dredged during USNS *Eltain* Marine Geology Cruises 16 and 37. Other dredge samples are detailed in Conway et al. (2012). Segmentations of the MRC are after Massell et al. (2000). The magenta arrows show the transform motions and directions of subduction of the MRC.. (c) Geological map of Macquarie Island, after Varne et al. (2000). New sample locations (dark blue circles) are annotated. The red squares indicate the sample locations of Kamenetsky et al. (2000), Kamenetsky and Maas (2002) and Husen et al. (2016).

2.3. Balleny Plateau, Tasman seamounts and Scott Plateau

In the vicinity of the MRC, several seamounts in the south Tasman Sea have been suggested to form the track of a hotspot now located beneath the Balleny Islands on the Antarctic plate, ~1000 km SE of Macquarie Island (Fig. 1a; Lanyon et al., 1993). Earlier activity of the Balleny hotspot produced the twin Heemskirk and Zeehan Seamounts with eruption ages estimated at ~70–60 Ma, the Janszoon Seamount at ~60–50 Ma in the south Tasman Sea and the Soela Seamount at ~40 Ma (Fig. 1a; Lanyon et al., 1993). The Balleny Plateau, including several islands, isolated reefs, and rock pinnacles, are interpreted as the most recent expression of the Balleny hotspot (Hart et al., 1997; Lanyon et al., 1993). The rocks from the Balleny province (Balleny Plateau and Tasman Seamounts) are mostly silica undersaturated rocks such as basanite, alkaline basalt, and trachybasalt. According to their enriched incompatible element patterns and isotope compositions ($^{206}Pb/^{204}Pb$ up to 20.727), these rocks are HIMU-like OIB (Lanyon et al., 1993).

A predominantly submarine plateau, which includes Scott Island, is located ~600 km to the east of the Balleny Islands and forms another volcanic edifice on the Antarctic Plate that could have been generated by a mantle plume (Fig. 1a; Lanyon et al., 1993). Dredged rocks from the submarine plateau are dominated by highly evolved rocks such as tephriphonolites and phonolites, with slightly more enriched incompatible element patterns and similar Sr, Nd and Pb isotopic compositions compared with rocks from Balleny Islands (Lanyon, 1994).

3. Sampling and analytical methods

3.1. Sampling strategy

Samples analyzed in this study include previously dredged rocks from seamounts from the submarine portion of the MRC and newly collected rocks from Macquarie Island (Fig. 1b, c). The dredged samples from the MRC seamounts were collected during the TAN0803 voyage in 2008 (Conway et al., 2012) and the USNS *Eltanin* Cruises 16 and 37 in 1965. The sampling locations encompass seven unnamed seamounts along the entire MRC, from Seamount 3 in the Puysegur Segment in the north (~50.1°S) to Seamount 10 in the Hjort Segment towards the south (~59.1°S; Fig. 1b). Samples were dredged using an epibenthic sled. We only chose rocks that were not rounded, showed limited alteration and no evidence of glacial transportation (e.g., striations) for further analyses as these were likely to have been sampled in situ. Samples from the MRC seamounts include basalts, glassy breccia, dolerite and gabbroic rocks (Conway et al., 2012).

A total of 23 rock samples were collected during an expedition to Macquarie Island in November 2017 from which a subset of ten basalt samples was selected for this study (Fig. 1c). Few samples have been collected from the southern parts of the island because promising sampling sites are remote (>30 km) from the base camp ANARE (Australian National Antarctic Research Expedition) located at the northern end of Macquarie Island, and are accessible only by foot over rugged terrain. Our sampling campaign focused on rocks from the upper oceanic crust, which covers three-quarters of the island (Fig. 1c). These rocks include basaltic flows, pillow lavas, rare tabular flows, and dykes found from the northernmost tip to the southern end of the island (Fig. 1c). Detailed petrographic descriptions of the samples are provided in the Supplementary Material.

3.2. Analytical methods

A total of 36 samples were selected for major and trace element analyses and 27 samples were selected for Sr–Nd–Pb isotope analyses. Major and trace elements were analyzed by X-ray fluorescence (XRF) and inductively coupled plasma mass spectrometry (ICP-MS), respectively. Strontium, Nd and Pb isotopic ratios were measured using a Thermo Neptune PLUS Multi-Collector ICP-MS at the University of Geneva. Detailed description of analytical methods are provided in the Supplementary Material.

4. Analytical results and observations

The new major and trace elements for the Macquarie Island samples and MRC seamount samples are reported in Supplementary Table 2, and the new Sr, Nd and Pb isotope data are reported in Table 1. Published geochemical data for the MRC, the Balleny Province, the Scott Plateau, and Deep Sea Drilling Project (DSDP) Sites 278 and 279 were compiled for comparative purposes (Supplementary Table 3).

Submarine basaltic rocks are susceptible to seawater alteration that is evidenced by high loss-on-ignition (LOI). Specifically, many major and few trace elements are likely mobilized by seawater when LOI is higher than 3 wt% (e.g., Caroff et al., 1995). The major and trace elements of the MRC seamount and Macquarie Island samples do not show obvious trend with LOI (Supplementary Fig. 2). However, the relatively mobile elements (e.g., K, Sr, Ba) of some samples that have high LOI (e.g., >2.5 wt%; Supplementary Fig. 2) show anomalously high values, indicating the influence of alteration. To make sure that only analytical data obtained from relatively fresh samples are used for geochemical interpretation, we only consider samples that have LOI <2.5 wt%. Plots of Nd and Pb isotopes vs LOI show no co-variation (Fig. 2). However, for Sr isotopes, there is a slight increase in Sr isotopic ratios with increasing LOI for the least radiogenic samples, which indicates that the Sr isotopic ratios could have been slightly affected by seawater alteration (Fig. 2), as Sr is relatively mobile during rock–seawater interactions (e.g., Mahoney et al., 1998). The lack of correlations between LOI and Nd and Pb isotopic ratios confirm that these elements are rather immobile during interactions with seawater. Therefore, we will rely on Nd and Pb isotopes in the discussion of the mantle source of the MRC samples.

The new samples from the MRC seamounts and Macquarie Island plot in the subalkaline series, close to the boundary with the alkaline series, in the total alkali–silica diagram (Fig. 3; Le Bas et al., 1986). Macquarie Island and the MRC seamount samples have similar compositions to samples from DSDP Sites 278 and 279 (Fig. 3; Pyle et al., 1995), which were also produced by the proto–Macquarie spreading ridge, but are different to the alkaline rocks of the Balleny province and Scott Plateau (Fig. 3).

Primitive mantle-normalized incompatible element patterns of new data from Macquarie Island and the MRC seamounts display continuous variation from a composition that is more enriched than N-MORB to a highly enriched MORB end-member that is more enriched than typical E-MORB (Fig. 4a, b). The MRC samples show positive anomalies in HFSE (high field strength elements: Nb, Ta, Zr) as well as strong negative K and Pb anomalies and moderate negative anomalies in Sr. The new data from the MRC samples display incompatible element patterns that show similarities with HIMU OIB from Cook–Austral Islands (Fig. 4a), as well as regional OIB of the Tasman Seamounts, Balleny Islands and Scott Plateau (Fig. 4b). However, different from those OIB-type basalts, the MRC samples show relatively flat heavy rare earth element (HREE) patterns (Fig. 4a, b).

Chondrite-normalized rare earth element (REE) patterns of the new MRC samples (except for the gabbro sample MRC-11) show flat to moderately enriched light vs heavy rare earth element (LREE/HREE) patterns, e.g., $(La/Sm)_{CN} = 0.95–3.11$, where $_{CN}$ = normalized to C1 chondrite (Sun and McDonough, 1989), and relatively flat HREE patterns (e.g., $[Dy/Yb]_{CN} = 1.04–1.34$). The La/Sm gradients are steeper than N-MORB and less steep than OIB, but the HREE slopes are similar to N-MORB and E-MORB and much flatter than those observed in OIB (Fig. 4c).

The seamount gabbro sample MRC-11 shows overall depletion in incompatible elements and relative enrichment in Sr and Eu (Fig. 4a, c), which is typical of plagioclase accumulation in oceanic gabbro

Table 1
Isotope analyses of basaltic rocks from the Macquarie Ridge Complex.

Sample	Sample type[a]	$^{143}Nd/^{144}Nd$	2SE[b]	$^{87}Sr/^{86}Sr$	2SE[b]	$^{206}Pb/^{204}Pb$	2SE[b]	$^{207}Pb/^{204}Pb$	2SE[b]	$^{208}Pb/^{204}Pb$	2SE[b]
Seamount 3											
MRC-5	Basalt	0.513028	0.000002	0.702953	0.000003	19.541	0.005	15.594	0.004	38.982	0.010
MRC-7	Basalt	0.513041	0.000002	0.702928	0.000003	18.991	0.005	15.524	0.004	38.502	0.010
MRC-8	Basalt	0.513034	0.000005	0.703172	0.000005	19.060	0.013	15.549	0.010	38.673	0.026
Seamount 5											
MRC-2	Basalt	0.513112	0.000003	0.702969	0.000005	18.547	0.009	15.456	0.008	38.042	0.019
MRC-9	Basalt	0.513030	0.000002	0.702925	0.000004	19.218	0.008	15.529	0.006	38.756	0.015
MRC-10	Basalt	0.513003	0.000003	0.702985	0.000005	19.084	0.008	15.587	0.007	38.758	0.017
MRC-11	Gabbro	0.513114	0.000011	0.703508	0.000007	18.252	0.018	15.504	0.015	37.867	0.037
Seamount 6											
MRC-12	Basalt	0.513050	0.000003	0.703026	0.000004	19.078	0.009	15.511	0.007	38.525	0.018
MRC-13	Basalt	0.513060	0.000003	0.703303	0.000004	19.095	0.004	15.529	0.004	38.568	0.009
MRC-14	Basalt	0.512964	0.000002	0.703258	0.000004	19.081	0.005	15.518	0.004	38.871	0.011
Seamount 7											
MRC-15	Basalt	0.513066	0.000003	0.703042	0.000004	18.958	0.009	15.516	0.007	38.545	0.017
MRC-16	Basalt	0.513079	0.000003	0.703054	0.000005	18.938	0.013	15.547	0.010	38.547	0.025
MRC-17	Basalt	0.513089	0.000003	0.703062	0.000005	18.904	0.010	15.495	0.008	38.511	0.020
Seamount 8											
MRC-18	Dolerite	0.513056	0.000003	0.703029	0.000004	18.847	0.019	15.408	0.016	38.212	0.039
MRC-19	Dolerite	0.513039	0.000003	0.703134	0.000004	18.946	0.034	15.592	0.028	38.587	0.071
Seamount 9											
MRC-22	Basalt	0.513092	0.000004	0.702927	0.000004	18.401	0.010	15.449	0.009	38.034	0.021
Seamount 10											
MRC-4	Dolerite	0.513069	0.000003	0.704173	0.000005	18.603	0.017	15.487	0.014	38.048	0.035
Macquarie Island											
MQ17-06	Basalt	0.513033	0.000004	0.704387	0.000003	19.228	0.011	15.560	0.008	38.783	0.020
MQ17-07	Basalt	0.513034	0.000003	0.703103	0.000003	19.282	0.006	15.559	0.005	38.820	0.013
MQ17-08	Basalt	0.513028	0.000002	0.703196	0.000003	19.295	0.006	15.584	0.005	38.866	0.012
MQ17-09	Glassy breccia	0.513063	0.000004	0.702867	0.000006	18.916	0.010	15.502	0.008	38.484	0.020
MQ17-10	Dolerite	0.513036	0.000002	0.703122	0.000004	19.378	0.012	15.563	0.010	38.896	0.024
MQ17-11	Dolerite	0.513012	0.000013	0.703024	0.000005	18.798	0.018	15.520	0.015	38.357	0.036
MQ17-12	Basalt	0.513092	0.000004	0.703159	0.000007	18.658	0.008	15.499	0.006	38.220	0.016
MQ17-13	Basalt	0.513069	0.000006	0.703743	0.000005	18.488	0.014	15.465	0.012	38.050	0.028
MQ17-14	Basaltic dyke	0.513045	0.000003	0.703112	0.000004	19.021	0.003	15.547	0.003	38.583	0.006
MQ17-15	Basaltic dyke	0.513084	0.000004	0.702798	0.000006	18.802	0.035	15.430	0.029	38.332	0.072

[a] Elemental concentrations of Rb, Sr, Sm, Nd, U, Th and Pb are available in Supplementary Table 3.
[b] Errors in 2 standard deviation.

(Coogan et al., 2001). In thin section, it is composed of plagioclase (60 vol%) and pyroxene (40 vol%) with a holocrystalline texture (Supplementary Fig. 1, Supplementary Table 1). Therefore, MRC-11 is a cumulate rock comprising of accumulations of plagioclase and pyroxene phenocrysts.

The new MRC samples show $^{87}Sr/^{86}Sr$ ranging from 0.70280–0.70417 and $^{143}Nd/^{144}Nd$ ranging from 0.51296–0.51311 (Fig. 5a, Table 1). The new samples have generally similar Sr isotopic ratios and Nd isotopic ratios to those previously analyzed in Macquarie Island glasses ($^{87}Sr/^{86}Sr$: 0.70257–0.70329, $^{143}Nd/^{144}Nd$: 0.51300–0.51306; Kamenetsky et al., 2000; Kamenetsky and Maas, 2002). In terms of Nd isotope ratios, the MRC basalts are similar to rocks from the Scott Plateau but are more radiogenic than rocks from the Balleny Plateau. Compared with MORB between the Pacific–Antarctic Ridge west of Udintsev Fracture Zone (~146°W) and the Southeast Indian Ridge east of Australian–Antarctic Discordance (~128°E; Fig. 1a, Supplementary Table 4), the MRC samples generally overlap in Sr and Nd isotope space, but also trend towards less radiogenic Nd isotopic compositions (Fig. 5a, b).

The new Pb isotope data from Macquarie Island and the MRC seamounts ($^{206}Pb/^{204}Pb$ = 18.252–19.541, $^{207}Pb/^{204}Pb$ = 15.408–15.594, $^{208}Pb/^{204}Pb$ = 37.867–38.982) generally overlap with previous data from the Macquarie Island glasses, but also extend towards less radiogenic compositions (Fig. 5b–d). There is no obvious difference between samples from the island (basalt and glass) and samples from the seamounts in terms of isotopic compositions. Overall, no systematic variation in isotopic ratios exists along the MRC (Supplementary Fig. 4).

In $^{207}Pb/^{204}Pb$ vs $^{206}Pb/^{204}Pb$ space, the new data from the MRC are more scattered than previous data, with a distribution towards lower $^{207}Pb/^{204}Pb$ and $^{206}Pb/^{204}Pb$ (Fig. 5c). However, the MRC samples show a strong positive correlation on the $^{208}Pb/^{204}Pb$ vs $^{206}Pb/^{204}Pb$ plot with a slope slightly shallower than that of the NHRL (Fig. 5d). Our new data show a strong affinity with the samples from DSDP Sites 278 and 279 (Fig. 5; Pyle et al., 1995), although the number of data from the two drilling sites are limited. Some of the MRC samples overlap with the Pacific–Indian MORB (MORB from the Pacific–Antarctic Ridge west of Udintsev Fracture Zone, and the Southeast Indian Ridge east of Australian–Antarctic Discordance; Figs. 1, 5), but the majority of them differ with lower $^{207}Pb/^{204}Pb$ at given $^{206}Pb/^{204}Pb$ (Fig. 5c), and higher $^{208}Pb/^{204}Pb$ and $^{206}Pb/^{204}Pb$ (Fig. 5d). The MRC samples together with the Macquarie Island glasses form a trend towards HIMU compositions similar to those of the Cook–Austral HIMU OIB (Fig. 5d). Such a trend is also observed for the Balleny Islands and Scott Plateau samples (Lanyon, 1994; Lanyon et al., 1993).

The MRC samples show a positive covariation between $(La/Sm)_{CN}$ and $^{206}Pb/^{204}Pb$, $^{207}Pb/^{204}Pb$ and $^{208}Pb/^{204}Pb$ (R^2 = 0.85, 0.50 and 0.80, respectively; Fig. 6a–c) and negative covariation with $^{143}Nd/^{144}Nd$, which is not as well defined as the other correlations (R^2 = 0.38; Fig. 6d). However, $(Dy/Yb)_{CN}$ do not show any covariation with any isotope ratios (R^2 = 0.08, 0.06, 0.06 and 0.14 for $^{206}Pb/^{204}Pb$,

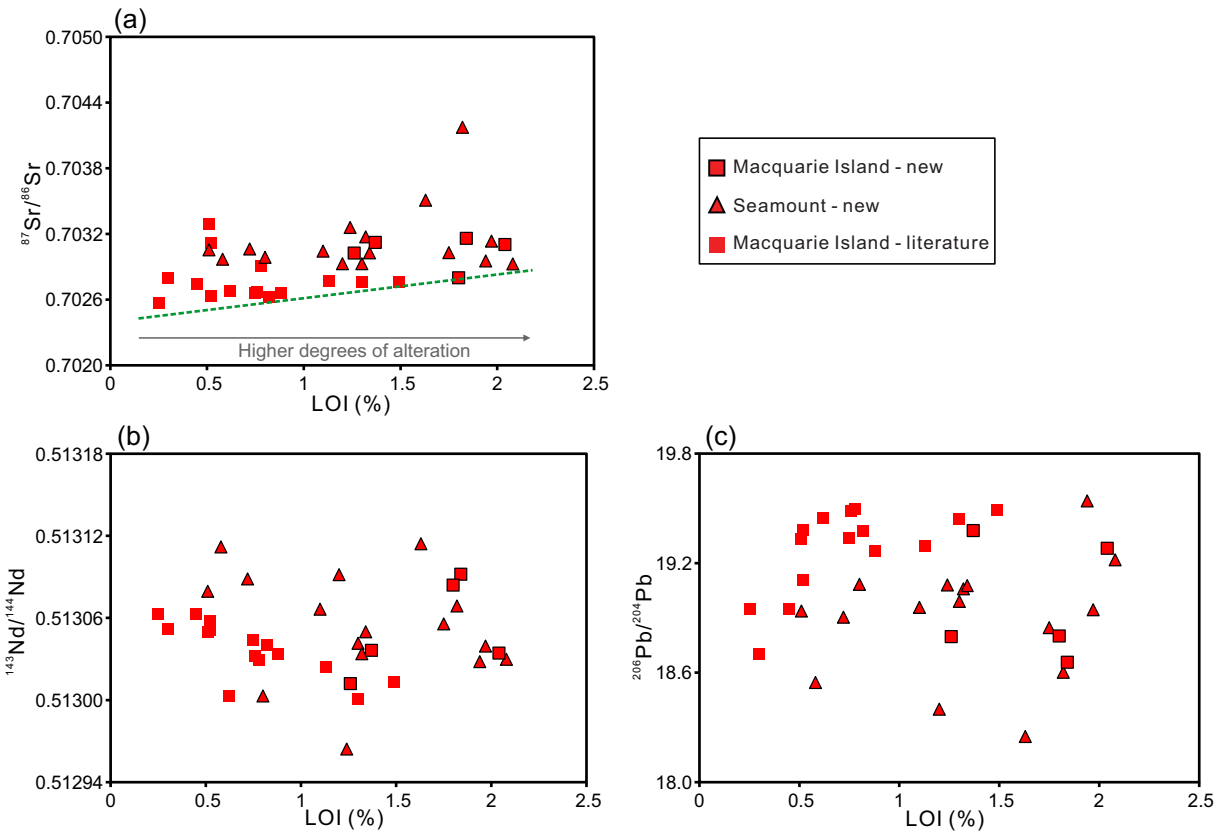

Fig. 2. Isotopic ratios vs LOI (Loss on ignition). The literature data for Macquarie Island are from Kamenetsky and Maas (2002). The data have been filtered for LOI <2.5%.

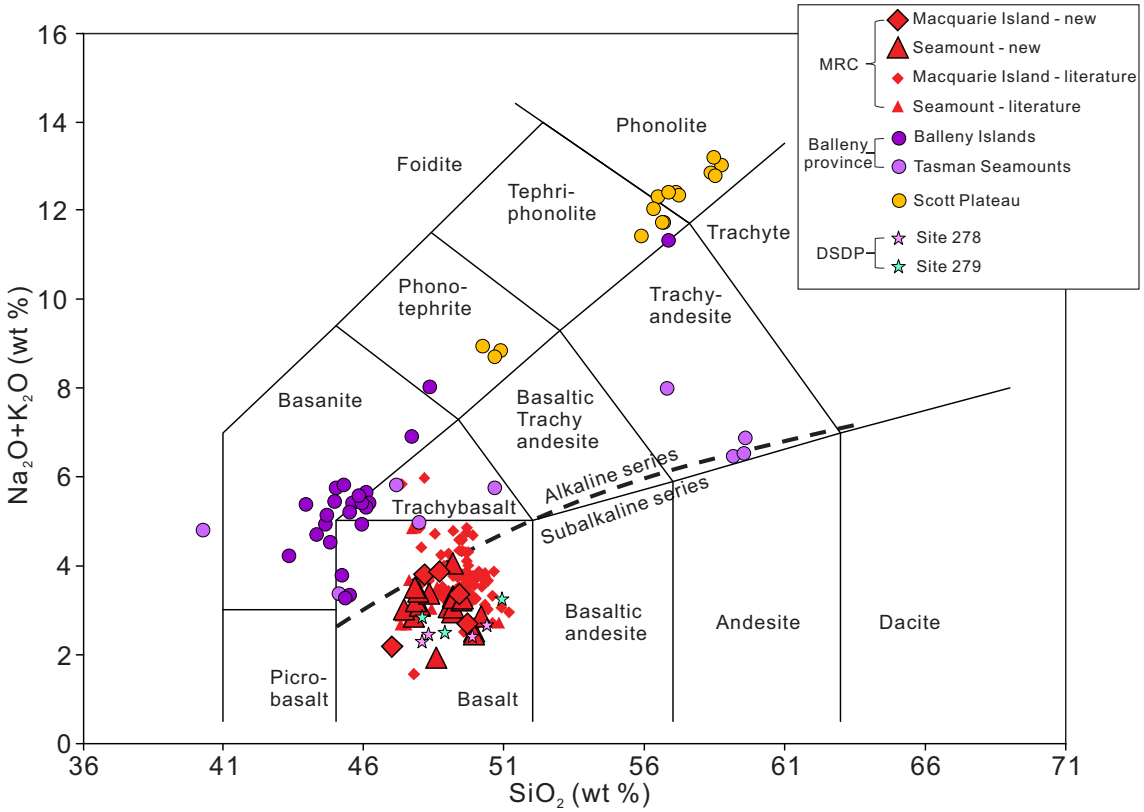

Fig. 3. Total alkali–silica diagram (TAS; Le Bas et al., 1986). The literature data are provided in Supplementary Table 3.

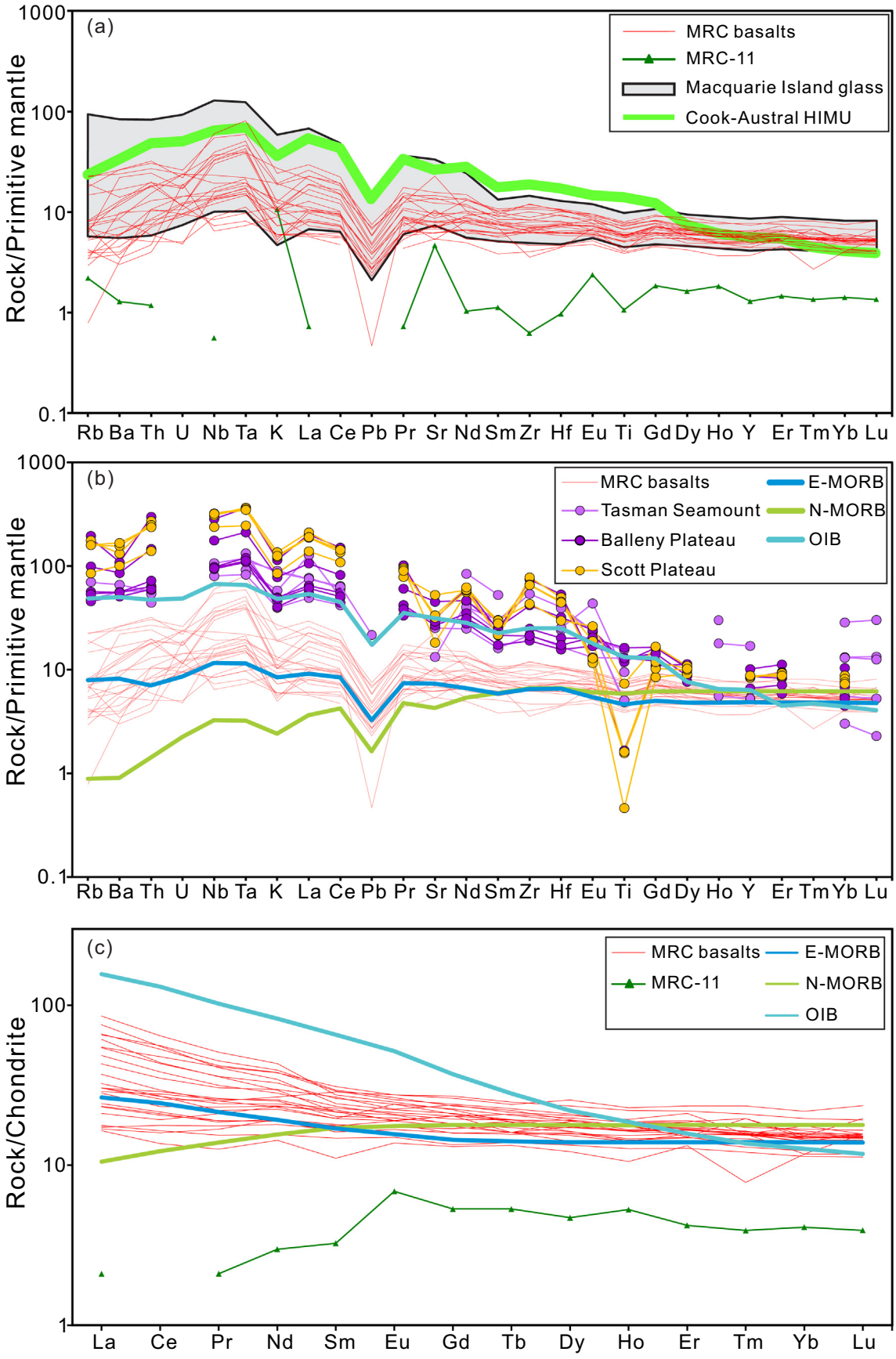
(a)
MRC basalts
MRC-11
Macquarie Island glass
Cook-Austral HIMU
Rock/Primitive mantle
1000
100
10
1
0.1
Rb Ba Th U Nb Ta K La Ce Pb Pr Sr Nd Sm Zr Hf Eu Ti Gd Dy Ho Y Er Tm Yb Lu
(b)
MRC basalts
Tasman Seamount
Balleny Plateau
Scott Plateau
E-MORB
N-MORB
OIB
Rock/Primitive mantle
1000
100
10
1
0.1
Rb Ba Th U Nb Ta K La Ce Pb Pr Sr Nd Sm Zr Hf Eu Ti Gd Dy Ho Y Er Tm Yb Lu
(c)
MRC basalts
MRC-11
E-MORB
N-MORB
OIB
Rock/Chondrite
100
10
1
La Ce Pr Nd Sm Eu Gd Tb Dy Ho Er Tm Yb Lu

$^{207}Pb/^{204}Pb$, $^{208}Pb/^{204}Pb$ and $^{143}Nd/^{144}Nd$, respectively; Fig. 6e–h). The MRC basalts show different patterns of REE ratios vs isotope ratios compared with the Balleny province samples (Fig. 6). Indeed, contrary to the MRC samples, the Balleny province samples have $(La/Sm)_{CN}$ and $(Dy/Yb)_{CN}$ that do not vary significantly regardless of the Pb and Nd isotopic ratios. Only three Sr–Nd–Pb isotope data are available from Scott Plateau, and they show limited variation of the isotopic ratios.

5. Discussion

5.1. Involvement of a mantle plume component in the MRC basalts?

Several lines of evidence suggest that MORB from the Macquarie Ridge Complex were not sourced from depleted and homogeneous upper mantle. These include: (i) Nd isotopes ratios mostly less radiogenic than those of N-MORBs; (ii) Pb isotopes extending beyond the MORB field towards a HIMU-like mantle component (Fig. 5); and (iii) similarities of the incompatible elements to those of regional HIMU OIB from the Balleny and Scott plateau samples, except for the relatively flat HREE patterns (Fig. 4). Therefore, the key issue to explain the geochemical and isotopic signatures of the MRC basalts is to determine whether these chemical features were caused by the contamination of a depleted upper mantle source by deep plume material, or they reflect heterogeneity of the upper mantle in the MRC region.

When a rising mantle plume encounters upwelling upper mantle at a spreading ridge, the isotopically-enriched plume material is entrained in the asthenosphere and the final melt isotopic compositions are intermediate between the plume and depleted asthenosphere and a chemical continuum can be observed between the depleted asthenosphere and enriched mantle plume endmembers. Such phenomenon has been observed, for example, at Iceland (e.g., Peate et al., 2010). The heterogeneous enrichment in incompatible elements (Fig. 4) and the observed trend formed by the MRC data from depleted MORB mantle (DMM) towards a HIMU-like component (Fig. 5), may suggest the involvement of a mantle plume and asthenospheric component in different proportions in the mantle source.

If a mantle plume component was responsible for the enriched nature of MRC melts, the purported Balleny mantle plume is the most probable plume source due to the relative geographical proximity between the MRC and the Balleny hotspot track (Fig. 1a), and the geochemical similarity between the MRC and Balleny basalts (Figs. 4, 5). Although the MRC basalts also show geochemical similarity to the Scott Plateau samples, which may have been produced by a mantle plume (Lanyon, 1994), the influence of an alleged Scott plume on the MRC is less likely due to a significant separating distance (> 1500 km, Fig. 1a). Moreover, there are only three isotopic data points from the Scott Plateau (Fig. 5), making any links to the MRC tentative at best.

We model the isotopic compositions of binary mixed melts derived from a depleted Pacific–Indian MORB source (DMM) and the Balleny plume source (Fig. 7a, b, c) to test whether the MRC basalts could have been produced by such mixed mantle source components. The isotopic compositions of the DMM and Balleny plume are heterogeneous to some extent (Fig. 5), so using just one 'representative' composition from each end-member in the mixing modelling would be inadequate to represent the isotopic characteristics of these end-members. To mitigate simplistic end-member compositions, we simulated 1000 possible compositions for each end-member to account for the range of their natural isotopic variations (Merle et al., 2017). To do this, one isotopic composition of each end-member was chosen and given a standard deviation (Gaussian) able to encompass the complete isotopic variations of basalt samples that has currently been studied for the mixing end-members (Fig. 7, Table 2). Then, using a Mersenne Twister random number generator associated with Monte Carlo simulations performed in QuantumXL, 1000, possible compositions that are normally distributed around the chosen mean composition are simulated. In each mixing simulation calculation, two isotopic compositions were randomly selected from each of the two theoretical end-member compositions, and were mixed in a random proportion (between 0 and 100%). This Monte Carlo simulation process was repeated for 1000 times and thus, 1000 mixed theoretical compositions were generated. The mixed theoretical isotopic compositions are more representative of the isotopic heterogeneity of mantle components that can be produced by solely mixing two 'representative' compositions from the end-members.

Our modelling results show that, in terms of Pb isotopes, the compositions of mixed melts derived from the Balleny mantle plume and the DMM have $^{208}Pb/^{204}Pb$ that are slightly too high to account for the MRC samples (Fig. 7b). Samples produced by the Balleny mantle plume have relatively high $^{208}Pb/^{204}Pb$ at given $^{206}Pb/^{204}Pb$ and lie close to the NHRL, while the majority of the MRC samples lie below the NHRL (Fig. 5d). These results suggest that the Balleny mantle plume was probably not involved in the generation of the MRC basalts.

5.2. Heterogeneous mantle source involving a mixture between DMM and HIMU components

The absence of evidence for direct contributions of plume material agrees with earlier interpretations on the mantle source of the Macquarie Island glasses (Kamenetsky et al., 2000). To account for the geochemical and isotopic heterogeneity of the Macquarie Island glasses, Kamenetsky et al. (2000) and Kamenetsky and Maas (2002) proposed a model involving the fractional 'dynamic' melting and efficient melt extraction of a single spinel-peridotite source, which itself is isotopically heterogeneous at the grain scale. The proposed peridotite mantle source was supported by the study of trace element compositions of olivine, clinopyroxene and melt inclusions in basalts and glasses from Macquarie Island (Husen et al., 2016), but was not supported by experiment-based modelling, which indicated that a mantle source richer in *Di* (diopside) and *JCL* (jadeite + calcium Tschermak's molecule + leucite) is required to generate the composition of the Macquarie Island glass (Varne et al., 2000). It is possible that the proposed peridotite mantle (Kamenetsky et al., 2000; Kamenetsky and Maas, 2002) is capable of preserving the Nd isotopic heterogeneity considering that grain-scale Nd isotopic heterogeneity can be preserved in plagioclase and clinopyroxene in lower crustal gabbros (Lambart et al., 2019) due to the extremely slow diffusion of Nd in these minerals (Van Orman et al., 2001). However, it is not clear whether these isotopic heterogeneities can be preserved at the solidus temperature of a peridotite. Even if the peridotite could retain the Sr, Nd and Pb isotopic heterogeneities, the proposed grain-scale isotopic heterogeneity of the peridotite makes it inconceivable to extract the melt in chemical isolation, and melt–solid diffusion can also modify the isotopic signatures (Lambart et al., 2019). Thus, fractional dynamic melting of a single spinel peridotite source (with efficient melt extraction) would be impossible to produce the isotopically enriched MORB-like basalts observed for the MRC samples.

Basalts from the two proximal Oligocene to Miocene DSDP Sites 278 (~26 Ma) and 279 (~15 Ma; Pyle et al., 1995; Fig. 1b) have similar elemental and isotopic compositions to the MRC (Figs. 1a, 5), with Site 279 having slightly more radiogenic isotopic compositions than Site 278. On isotope vs incompatible element ratio plots, Sites 278 and 279

Fig. 4. (a) Primitive mantle normalized incompatible element patterns for the MRC samples. The Macquarie Island glasses data are from Kamenetsky et al. (2000) and Wertz (2003). Data for Cook–Austral Islands are from the GEOROC database (http://georoc.mpch-mainz.gwdg.de/georoc/Start.asp). (b) Primitive mantle normalized incompatible element patterns for the MRC, Tasman Seamounts, Balleny Islands and Scott Island. (c) Chondrite normalized rare earth element patterns for the new MRC samples. Data for N-MORB, E-MORB and OIB, and all normalization values, are from Sun and McDonough (1989). The data have been filtered for loss-on-ignition (LOI <2.5%).

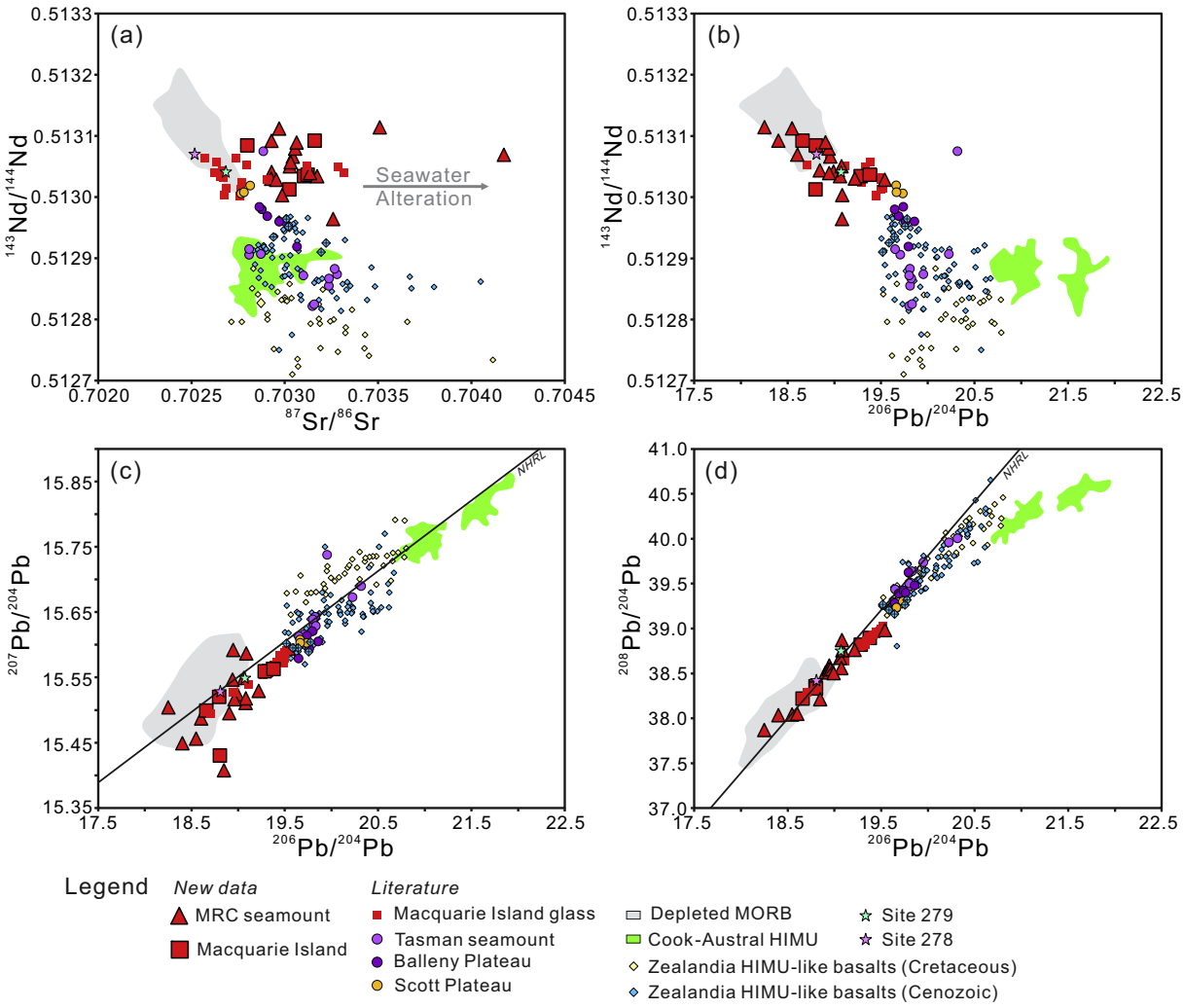

Fig. 5. Isotopic compositions of the MRC samples and related volcanism products. The Cenozoic Zealandia HIMU-like basalts from the western Campbell Plateau are represented by blue diamonds with thick boundary and cross inside. Previous data for the Macquarie Island glasses are from Kamenetsky et al. (2000) and Kamenetsky and Maas (2002). NHRL—Northern Hemisphere Reference Line (Hart, 1984). Data for the Balleny Islands are from Hart (1988), Lanyon et al. (1993) and Lanyon (1994); Data for the Scott Plateau and DSDP drill sites are from Lanyon et al. (1993), Lanyon (1994) and Pyle et al. (1995); The depleted MORB are from the Pacific–Antarctic Ridge west of Eltanin Fracture Zone, and the Southeast Indian Ridge east of Australian–Antarctic Discordance. Zealandia HIMU-like basalts are from the South Island of New Zealand, the submarine Campbell Plateau (including Auckland, Antipodes and Campbell Islands), Chatham Rise, Challenger Plateau, and seamounts on the Hikurangi Plateau (Supplementary Table 4). Data for the Cook–Austral Islands are from the GEOROC database (http://georoc.mpch-mainz.gwdg.de/georoc/Start.asp). The isotope data have been filtered for loss-on-ignition (LOI <2.5%). The uncertainty on individual analyses are smaller than the plotted symbols.

lie on the trends defined by the MRC (Fig. 6). Considering that basalts from these two sites are earlier products of the proto–Macquarie spreading ridge, this may suggest that the chemical composition of the mantle source underneath the spreading centre has not significantly changed since the inception of the proto-Macquarie spreading ridge at ~40 Ma, although more age and isotope data are still needed. Thus, the isotopic signature of the MRC basalts is, most likely, not a small chemical heterogeneity localized to a specific region, but rather a long-term and large-scale chemical anomaly in the vicinity of the Australian–Pacific (−Antarctic) plate boundary (Fig. 1).

Widespread Cretaceous–Cenozoic intraplate volcanism on the Zealandia continent generated magmatism with HIMU-like isotopic signatures, including continental basaltic volcanism on the South Island of New Zealand, and oceanic volcanism on the submarine Campbell Plateau (including Auckland, Antipodes and Campbell Islands), Chatham Rise, Challenger Plateau, and seamounts on the Hikurangi Plateau (Fig. 5, Supplementary Table 4; Hoernle et al., 2010; Hoernle et al., 2020; Hoernle et al., 2006; McCoy-West et al., 2010; Timm et al., 2010; Van der Meer et al., 2017). The chemical characteristics of the Cretaceous Zealandia intraplate HIMU-like basalts have been interpreted as derived from a deep-seated mantle plume (Hoernle et al., 2020) while the Cenozoic lavas may have been formed by decompression melting of upwelling asthenosphere triggered by delamination of small portions of cool and dense subcontinental lithospheric keel in response to gravitational instabilities along the lithospheric–asthenospheric mantle boundary (Hoernle et al., 2006; Timm et al., 2010). The isotopic compositions of the MRC basalts seem to trend towards that of the Cenozoic series of the Zealandia HIMU-like basalts, and are different from the Cretaceous lavas in having lower $^{207}Pb/^{204}Pb$ at given $^{206}Pb/^{204}Pb$ (Fig. 5c). Therefore, it is likely that there is a shared origin in mantle components between the MRC basalts and the Cenozoic Zealandia HIMU-like basalts considering their geochemical similarities and close proximity (Fig. 1a).

We model the isotopic compositions of mixed melts derived from a DMM and a Cenozoic Zealandia HIMU-like mantle source (Fig. 7d–f). A similar Monte Carlo simulation was applied to this modelling as outlined in section 5.1. Considering that there is significant regional heterogeneity in the compositions of the HIMU-like basalts in Zealandia

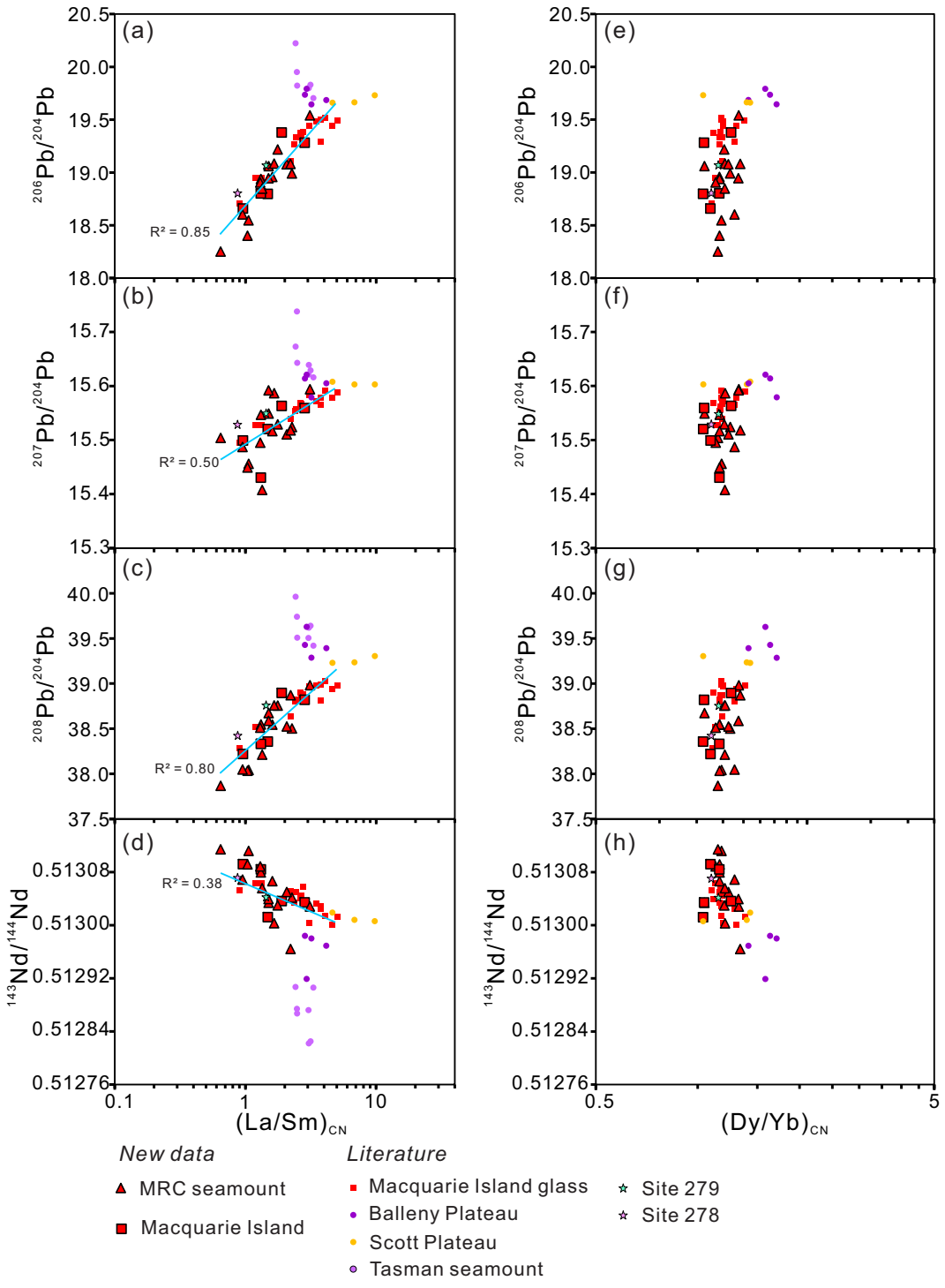

Fig. 6. Isotopic ratios vs REE ratios, with REE ratios normalized to chondrite after Sun and McDonough (1989). The blue solid lines indicate linear regressions of the MRC samples.

(Fig. 5), we use the compositions of basalts from the nearest part of Zealandia to the MRC as the HIMU-like component in the mixing modelling, specifically from Auckland Island, Campbell Island and Pukaki Bank from the western Campbell Plateau (Figs 1a, 5, Table 2, Supplementary Table 4). The modelling results show that both Nd and Pb compositions of the MRC samples can be generated by mixing a depleted MORB mantle component with a Cenozoic Zealandia HIMU-like component. We note that there are few MRC samples having relatively low $^{143}Nd/^{144}Nd$ ($n = 1$) or high $^{143}Nd/^{144}Nd$ ($n = 2$) at given $^{206}Pb/^{204}Pb$ which cannot be satisfactorily modelled (Fig. 7f). This suggests that the actual HIMU-like mantle source component could be slightly more heterogeneous than what was currently sampled from basalts on the western Campbell Plateau. However, these few outliers do not affect the implications of the modelling that the MRC basalts and the Cenozoic Zealandia (particularly the western Campbell Plateau) HIMU-like basalts may thus share similar mantle source components.

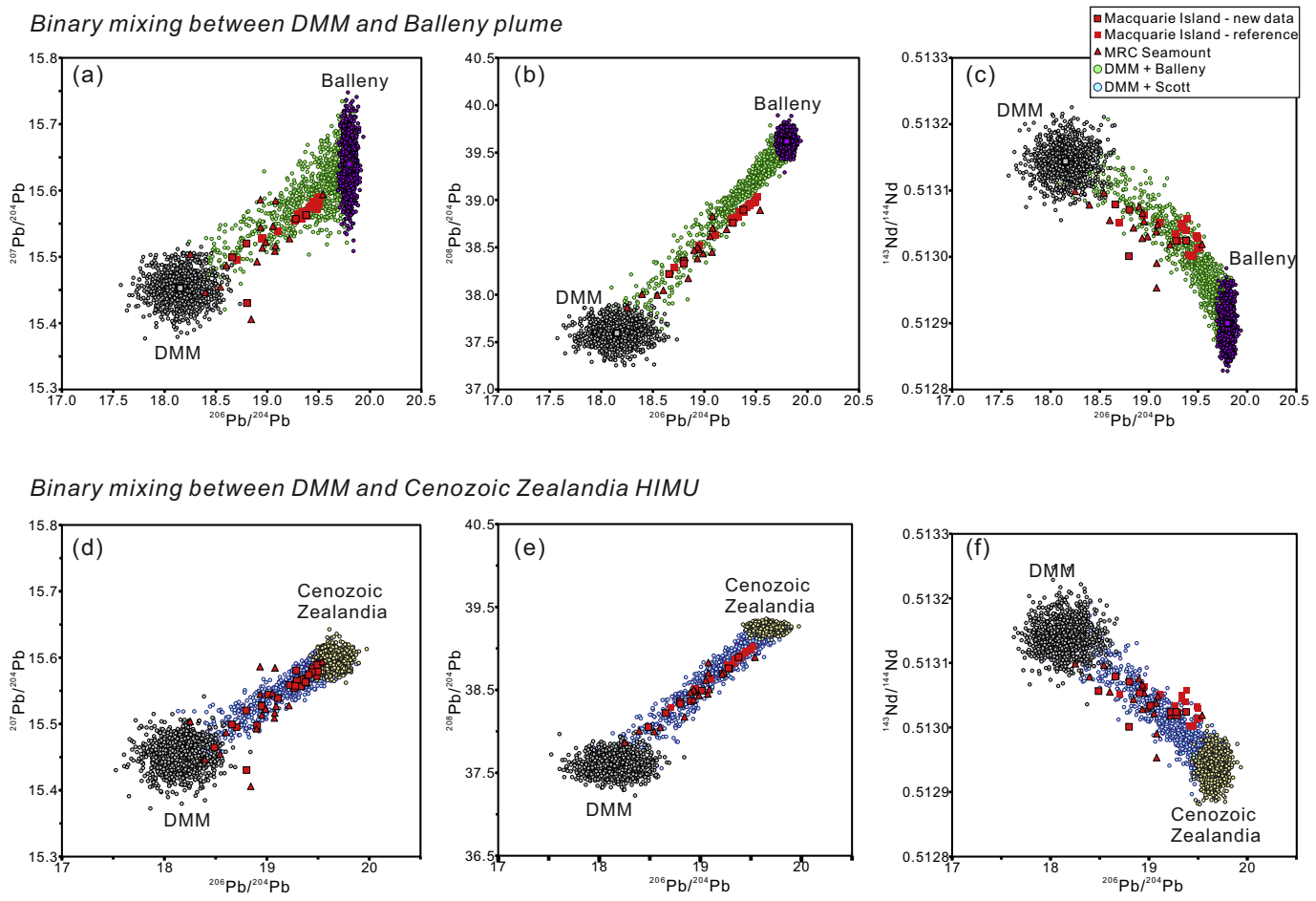

Fig. 7. Numerical modelling of binary mixing between the depleted MORB mantle (DMM) source and the (a, b, c) Balleny plume, and (d, e, f) Cenozoic Zealandia HIMU. The possible isotopic compositions of the source of the MRC basalts were calculated using a Monte Carlo simulation approach and 1000 trials were conducted for each simulation. The compositions and uncertainties of the mixing source components are in Table 2.

5.3. Origin of the enriched mantle component

The models discussed above indicate the presence of an isotopically enriched component in the mantle source of the MRC basalts, possibly sharing an origin with the HIMU-like component found in the western Campbell Plateau portion of the Zealandia microcontinent. The origin of the isotopically enriched mantle signature presented in the Macquarie Island glasses remains unclear. The formation of HIMU basalts has generally been attributed to recycling of altered, subducted oceanic crust within mantle plumes rising from the deep mantle (e.g., Stracke et al., 2005). However, a recycled oceanic crust component in the mantle source of MRC basalts was not supported by the MORB-like $^{3}He/^{4}He$ and high Br/Cl of the Macquarie Island glasses (Kendrick et al., 2012), while a plume component from the Balleny mantle plume is unsupported by the Monte Carlo mixing modelling results (Fig. 7).

Alternatively, HIMU-like isotopic and geochemical signatures of oceanic basalts could be generated by metasomatised continental or oceanic lithospheric mantle (e.g., Homrighausen et al., 2018; Scott et al., 2016). The Monte Carlo mixing modellings reveal affinity in the isotopically enriched component between the MRC basalts and Cenozoic Zealandia HIMU-like basalts (Fig. 7). Given that the HIMU-like signatures of the Cenozoic Zealandia basalts have been attributed to partial melting of metasomatised sub-continental lithospheric mantle (Hoernle et al., 2006; McCoy-West et al., 2010; Panter et al., 2006; Timm et al., 2010), we explore in the following section whether such a component could also contribute to the source of the heterogeneous mantle signature of the MRC basalts.

The new data for the MRC basalt samples and previous data for the Macquarie Island glass samples show significant variation in the abundance of REE (e.g., $[La/Sm]_{CN} = 0.95–5.07$) and other incompatible

Table 2
The mean and standard deviations of isotopic compositions of melts derived from the end-member mantle sources.

End-members	Nd (ppm)[a]	$^{143}Nd/^{144}Nd$[b]	Pb (ppm)[a]	$^{206}Pb/^{204}Pb$[b]	$^{207}Pb/^{204}Pb$[b]	$^{208}Pb/^{204}Pb$[b]
Depleted MORB (P)	14.0 ± 3%	0.513144 ± 0.005%	0.68 ± 1%	18.152 ± 1%	15.453 ± 0.15%	37.596 ± 0.3%
Balleny plume (B)	33.7 ± 10%	0.512822 ± 0.005%	4.0 ± 2%	19.799 ± 0.2%	15.639 ± 0.24%	39.619 ± 0.2%
Zealandia HIMU (Z)	46.34 ± 3%	0.512937 ± 0.004%	2.80 ± 1%	19.655 ± 0.4%	15.597 ± 0.07%	39.244 ± 0.1%

[a] Average values of basalts produced by the end-member mantle sources (compiled data are available in Supplementary Tables 3–4).
[b] Note that the isotopic compositions and uncertainties are not from a specific sample of the endmember components, but are used to generate isotopic composition fields to encompass the variations of the endmember components.

trace elements (Fig. 4). Slight enrichment in the LREE and MREE to HREE ratios, such as Dy/Yb or Sm/Yb, has often been attributed to the presence of residual garnet in a MORB source (Hirschmann and Stolper, 1996; Waters et al., 2011). Global compilations of $(Sm/Yb)_{DM}$ ($_{DM}$ = normalized to depleted mantle; Hirschmann and Stolper, 1996) of N-MORB range from 1.31–1.49 (Hofmann, 1988). The $(Sm/Yb)_{DM}$ of the MRC basalts range from 1.36–3.79 (average = 2.15), which are higher than normal MORB values and may indicate the existence of residual garnet in the mantle source of MRC basalts. This is also supported by the $(Tb/Yb)_{CN}$ of the MRC basalts (1.01–1.59; average = 1.27; Supplementary Table 2), which is higher than that of typical N-MORB and E-MORB ($(Tb/Yb)_{CN}$ = 1.0; Sun and McDonough, 1989; Wang et al., 2002).

The negative anomalies of alkali elements (e.g. Ba, K) of the new MRC samples (Fig. 4) may require the presence of phlogopite or amphibole in the mantle source because, relative to normal anhydrous mineral melting, the involvement of amphibole or phlogopite during partial melting would result in the retention of alkali elements and water (Adam et al., 1993). The trends towards lower K/La for higher La contents and higher La/Yb, and a lack of trend in the Ba/La vs La and Ba/La vs La/Yb plots (Supplementary Fig. 5) indicate amphibole rather than phlogopite was the dominant hydrous mineral in the mantle source (Haase et al., 2004). The presence of amphibole-bearing mantle has been proposed as the source of HIMU-like basalts for Zealandia, including the Lookout Volcanics (McCoy-West et al., 2010), the Antipodes, Campbell and Chatham Islands (Panter et al., 2006), and lamprophyre dikes from Westland (Van der Meer et al., 2017).

Previously, a garnet-free, spinel peridotite was proposed to be the mantle source of the Macquarie Island glasses due to the relatively unfractionated HREE compositions (Kamenetsky and Maas, 2002), and the La/Sm vs Gd/Yb of the Macquarie Island glasses were subsequently used to define a garnet-free melting trend for MORB (Fig. 4 of Kamenetsky and Eggins, 2012). However, the modelling results of Waters et al. (2011) suggested that large proportions (>95%) of melts of N-MORB composition mixed with small proportions (<5%) of garnet pyroxenite melts are able to produce the incompatible element patterns of E-MORB (with relatively flat HREE patterns; Fig. 12 of Waters et al., 2011). The relatively flat HREE of the MRC basalts could be explained by the co-existence of residual garnet and amphibole in the mantle source. While garnet strongly partitions HREE, amphibole is the only common mantle-bearing mineral where MREE are preferentially incorporated over LREE and HREE (Dalpé, 1994; Tiepolo et al., 2007).

We model the REE ratios of the MRC by melting three possible mantle sources: spinel lherzolite, garnet lherzolite and amphibole-bearing garnet pyroxenite. As fixed parameters of the partial melting model, we used the REE partition coefficients of McKenzie and O'Nions (1991), and the equations of Shaw (1970), which quantitatively described trace element fractionation during fractional melting. Other parameters required in the modelling include the REE compositions and modal compositions of the mantle source, and the melting modes (proportions of the melting phases; Table 3). The peridotites exposed on Macquarie Island show highly refractory signatures suggesting they are residues after high degree of partial melting (Dijkstra et al., 2010; Wertz, 2003). Conversely, the basalts on Macquarie Island show enriched characters and require low overall degrees of partial melting of the mantle source and thus cannot be generated from the refractory peridotites on the island. In addition, no mantle xenolith has been found in the MRC basalts. Therefore, the lithology and geochemical composition of the source of the MRC basalts, as well as the proportions of the melting phases, are uncertain. In spite of the source uncertainty, we chose theoretical compositions and melting mode from the literature for the spinel peridotite (Niu, 1997; Thirlwall et al., 1994), garnet peridotite (Thirlwall et al., 1994; Walter, 1998) and amphibole-bearing garnet pyroxenite (McCoy-West et al., 2010).

Partial melting modelling results of the three mantle sources are presented in Fig. 8. Although some of the MRC basalts can be adequately modelled by partial melting of spinel peridotite source, the majority of the MRC basalts have excessively high La/Yb and La/Sm that cannot be generated by melting spinel-bearing peridotite alone. Small amounts of garnet are required in the mantle source to yield the observed LREE/HREE (e.g., La/Yb) and MREE/HREE patterns (e.g., Eu/Yb, Gd/Yb).

Partial melting modelling of a garnet-bearing peridotite shows that most of the MRC basalts cannot be produced by such a source due to their relatively low Gd/Yb (Fig. 8). In addition, if partial melting begins in the garnet peridotite field (~70–90 km depth), the oceanic crust produced would be greater (>10 km; cf. Fig. 1 in Hirschmann and Stolper, 1996) than the normal thickness of 7 ± 1 km (2σ) formed entirely within shallow crustal depths associated with MORB production (e.g., Klein and Langmuir, 1987). Using the 1 × 1° global crustal thickness model CRUST1.0 of Laske et al. (2013), we calculate a thickness of 7.2 ± 0.7 km (2σ) for the oceanic crust generated by the proto-Macquarie spreading centre (from 154.5°E to 162.5°E and − 51.5°S to −58.5°S), indicating that there is no anomalously thick oceanic crust in this region. This also suggests that the MRC basalts were not produced by melting in the garnet peridotite stability field at depths greater than ~70–90 km.

The MRC samples lie close to the partial melting curves of amphibole-bearing garnet pyroxenite (Fig. 8). To account for the presence of garnet but the lack of anomalously thick oceanic crust, we argue that the MRC basalts were derived from a predominantly spinel peridotite source, with small amounts of amphibole-bearing garnet pyroxenite. Although MORBs are believed to be derived from relatively shallow source regions (<70 km) in the stability field of spinel

Table 3
Parameters used in the partial melting modelling.

	Spinel lherzolite		Garnet lherzolite		Amphibole–garnet pyroxenite	
	Modal composition	*Melting mode*	*Modal composition*	*Melting mode*	*Modal composition*	*Melting mode*
Olivine	0.578	−0.167	0.658	0.07	0.04	0.025
Orthopyroxene	0.27	0.466	0.211	−0.16	0.70	0.20
Clinopyroxene	0.119	0.652	0.115	0.68	0.11	0.205
Spinel	0.033	0.049				
Garnet			0.02	0.25	0.04/0.02	0.25
Amphibole					0.08	0.315
References	Thirlwall et al., 1994	Niu, 1997	Thirlwall et al., modified	Walter, 1998	McCoy-West et al., 2010, modified	McCoy-West et al., 2010
REE compositions						
La (ppm)	0.687		0.70		0.69	
Sm (ppm)	0.444		0.34		0.32	
Eu (ppm)	0.172		0.162		0.168	
Gd (ppm)	0.596		0.54		0.56	
Yb (ppm)	0.4		0.53		0.515	

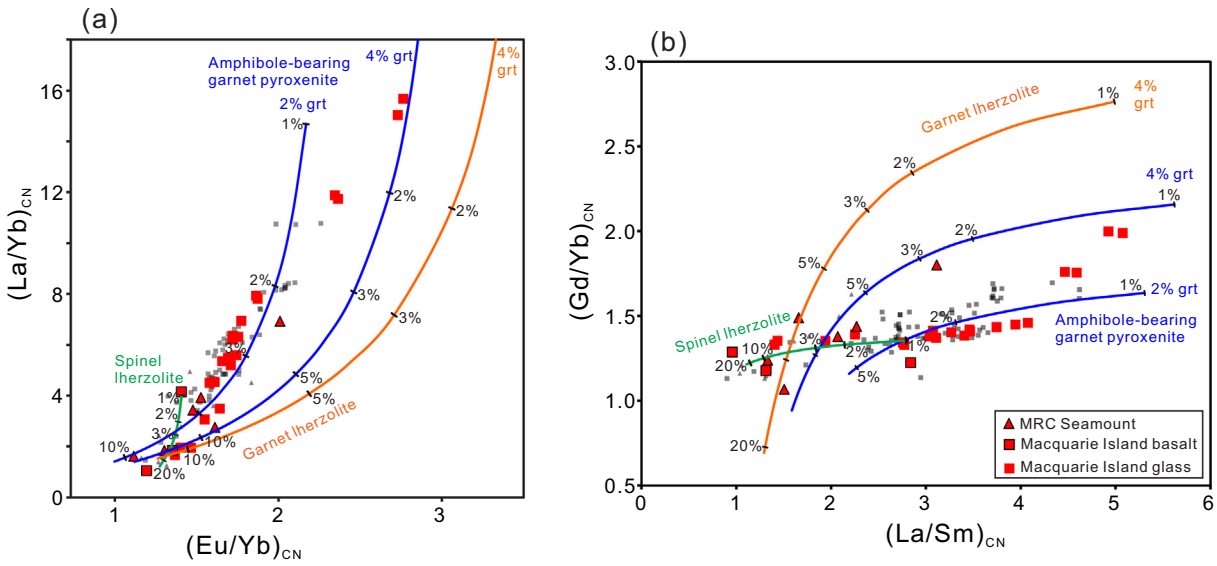

Fig. 8. (a) $(La/Yb)_{CN}$ vs $(Eu/Yb)_{CN}$ and (b) $(Gd/Yb)_{CN}$ vs $(La/Sm)_{CN}$ for the MRC basalts and fractional batch melting modelling of a spinel lherzolite, a garnet lherzolite and an amphibole-bearing garnet pyroxenite mantle source. The red symbols represent near-primitive Macquarie Island basaltic glasses and new samples with MgO > 8.0 wt%, and the semi-transparent grey symbols represent fractionated Macquarie Island basaltic glasses (Kamenetsky et al., 2000) and new samples that have MgO < 8.0 wt%. These two group of samples do not show systematic difference, indicating that fractional crystallisation should not noticeably affect the REE ratios. Values are chondrite-normalized after Sun and McDonough (1989). The parameters used in the modelling are presented in Table 3. The tick marks on the curves correspond to degrees of partial melting.

(O'Hara et al., 1971), garnet is stable at lower pressures in pyroxenite than in peridotite (Hirschmann and Stolper, 1996). Pyroxenite has a lower melting temperature than peridotite and begins to melt at greater depths than the surrounding peridotite (Hirschmann and Stolper, 1996; Ito and Mahoney, 2005; Lambart et al., 2009). Thus, early stages of melting will melt pyroxenite preferentially. If this pyroxenite entrained into dominantly peridotitic mantle has HIMU isotope characteristics (e.g., Hamelin and Allègre, 1988; Morgan, 1999), then it would be expected that basalts produced by lower degrees of partial melting would have higher proportions of HIMU to MORB melts (i.e., higher pyroxenite to peridotite melts, respectively). The $(La/Sm)_{CN}$ acts as a good proxy for partial melting degree, with higher ratios indicative of smaller degrees of melting. $(La/Sm)_{CN}$ could also vary as a result of direct mixing between enriched and depleted melts, but this would also generate covariations between $(Dy/Yb)_{CN}$ and isotope ratios, which are not observed (Fig. 6e–h). In the MRC basalts, positive covariations between $(La/Sm)_{CN}$ and Pb isotopes, and negative correlations between $(La/Sm)_{CN}$ and Nd isotopes (Fig. 6a–d) therefore support the presence of fertile HIMU-like pyroxenitic components in a dominantly peridotitic source. At shallower depths in the melting column, the spinel peridotite would begin to melt and the ratio of peridotite to pyroxenite would increase with increasing degrees of partial melting. The less radiogenic but significantly more voluminous peridotitic melts would then obscure the geochemical signature of the smaller amount of more radiogenic pyroxenite melts, yielding overall lower Pb isotopic ratios with increasing degrees of partial melting. Thus, the incorporation of small proportions of pyroxenite, potentially present as veins in a dominantly peridotitic mantle, is supported by trace element vs isotopic ratio plots (Fig. 6).

The presence of small portions of pyroxenite within largely peridotitic mantle also circumvents the issue of the dynamic melting model previously proposed for the Macquarie Island glasses (Husen et al., 2016;Kamenetsky et al., 2000 ; Kamenetsky and Maas, 2002). The main issue with dynamic melting of a grain-scale heterogeneous mantle source (Kamenetsky et al., 2000; Kamenetsky and Maas, 2002) is that it cannot satisfactorily explain how the isotopically enriched melts (generated by isotopically enriched 'grains') were extracted in chemical isolation with isotopically depleted melts (generated by isotopically depleted 'grains') to form isotopically enriched glass samples. Moreover, this model also does not explain how the grain-scale heterogeneity of the mantle source managed to survive melt–solid diffusion (Lambart et al., 2019). In our pyroxenite-veined mantle model, pyroxenite and peridotite can generate their own network of channels and experience limited magma mixing inside the channels (Lambart et al., 2019). The melt–rock reaction between pyroxenite-derived melts and the surrounding peridotite is also limited and thus the pyroxenite-derived melts are able to preserve their geochemical and isotopic characteristics en route to the lower crust (Lambart et al., 2012). Various proportions of pyroxenite-derived melts and peridotite-generated melts can then be mixed together to form geochemically and isotopically heterogeneous basalts. Again we note that the limited amount of amphibole-bearing garnet pyroxenite (<5%) will not cause an obvious rise in the Dy/Yb and Gd/Yb ratios for the MRC samples based on our modelling results (Fig. 8b) and that of Waters et al. (2011). This model is consistent with the recent finding that the variations in the isotopic compositions of MORB are caused by the different proportions of recycled material in the aggregated magma (Lambart et al., 2019). A similar pyroxenite-veined peridotite mantle source has previously been proposed to explain the elongate tube-like field in isotopic space of OIB (Morgan, 1999).

5.4. Origin of pyroxenite veins in the shallow mantle

Previous studies have demonstrated that pyroxenite veins could be formed within the metasomatised lithospheric mantle (e.g., Niu and O'Hara, 2003) and that amphibole in the pyroxenite veins could be formed by infiltration of carbonatitic or hydrous fluids, or low-degree partial melts of subducted oceanic lithosphere, into a peridotitic mantle (Yaxley et al., 1991). Considering that amphibole is not stable and can break down easily at the temperature of the convecting asthenospheric mantle (Yaxley and Kamenetsky, 1999), the pyroxenite veins most likely reside in the oceanic lithospheric mantle.

The Monte Carlo mixing modelling revealed isotopic affinity between the MRC basalts and the Cenozoic Zealandia HIMU-like basalts (Fig. 7d–f). The HIMU-like isotopic and geochemical signatures of the

Cenozoic Zealandia basalts are believed to be derived from a SCLM that was metasomatised by melts or fluids originated from subducted slabs along the east Gondwana subduction margin (Fig. 9; McCoy-West et al., 2010; Panter et al., 2006; Timm et al., 2010; Van der Meer et al., 2017). We posit that the bottom of the oceanic lithospheric mantle under the Macquarie Basin (Figs. 1b, 9) was similarly metasomatised by melts and/or fluids derived from subduction-related material in the asthenosphere, which is supplied by ancient and/or recent subduction along the Pacific margin before the breakup of East Gondwana (Larter et al., 2002). Alternatively, if not directly metasomatised by subduction-related material, the Macquarie Basin oceanic lithospheric mantle could be influenced by the fluids or partial melts of the delaminated Zealandia metasomatised SCLM (Fig. 10; Hoernle et al., 2006). The fluids or melts of the metasomatised SCLM could be transferred to the base of the Macquarie Basin oceanic lithosphere by the lateral and vertical flow of warm Pacific mantle, which was triggered by Rayleigh–Taylor instabilities due to the sudden detachment and sinking of subducted slabs along the former Gondwana margin (Fig. 9; Finn et al., 2005), or by the upper mantle instability induced by the strike-slip motion of the Macquarie Ridge (Massell et al., 2000; Mosher and

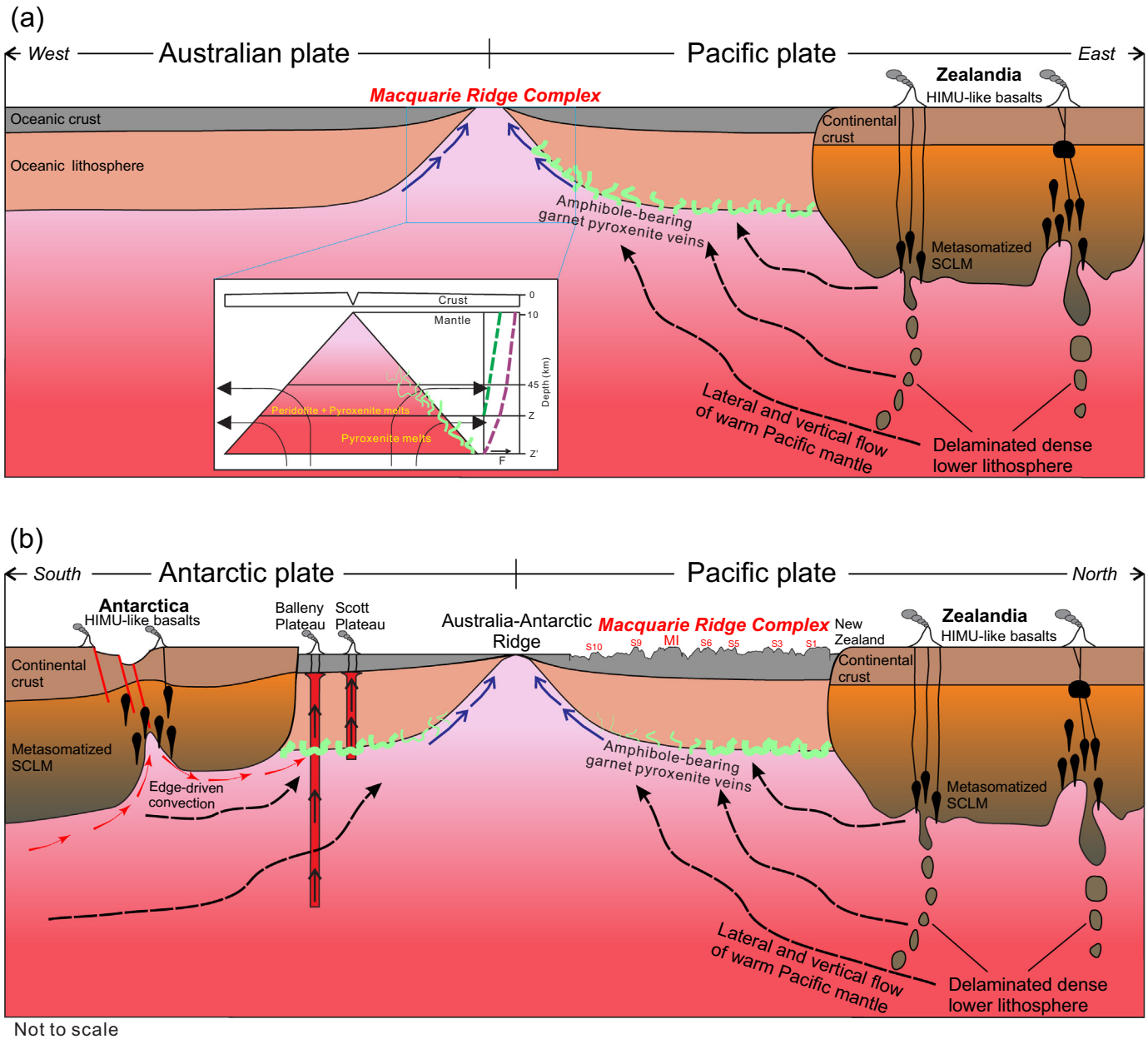

Fig. 9. Schematic illustrations of the mantle sources of the Macquarie Ridge Complex, Balleny Plateau and Scott Plateau. (a) West to east profile across the Australian plate, Macquarie Ridge Complex and Pacific plate. (b) South to north profile across the Antarctic plate, Australia–Antarctic Ridge and Pacific plate. Insert in (a) schematically shows melting of a pyroxenite-veined peridotitic upper mantle beneath the Macquarie Ridge after Hirschmann and Stolper (1996). The pyroxenite has a greater depth of solidus (Z') than the peridotite (Z). The dashed lines indicate the degrees of partial melting (F) reached for the peridotite (green) and pyroxenite (purple) as a function of depth. Melts generated by lower degrees of partial melting at greater depths would incorporate more pyroxenite-derived components, and therefore have a more noticeable HIMU-signature. The formation of the basalts in Zealandia was triggered by delamination of the SCLM and subsequent upwelling and related decompression melting according to Hoernle et al. (2006). The formation of the Antarctic basalts was triggered by crustal extension and edge-driven convection of the upper mantle (Panter et al., 2018). The HIMU-like components in the basalts were provided by metasomes in the lithospheric mantle, which were formed by the fluids and/or melts of subducted slab along the former east Gondwana margin.

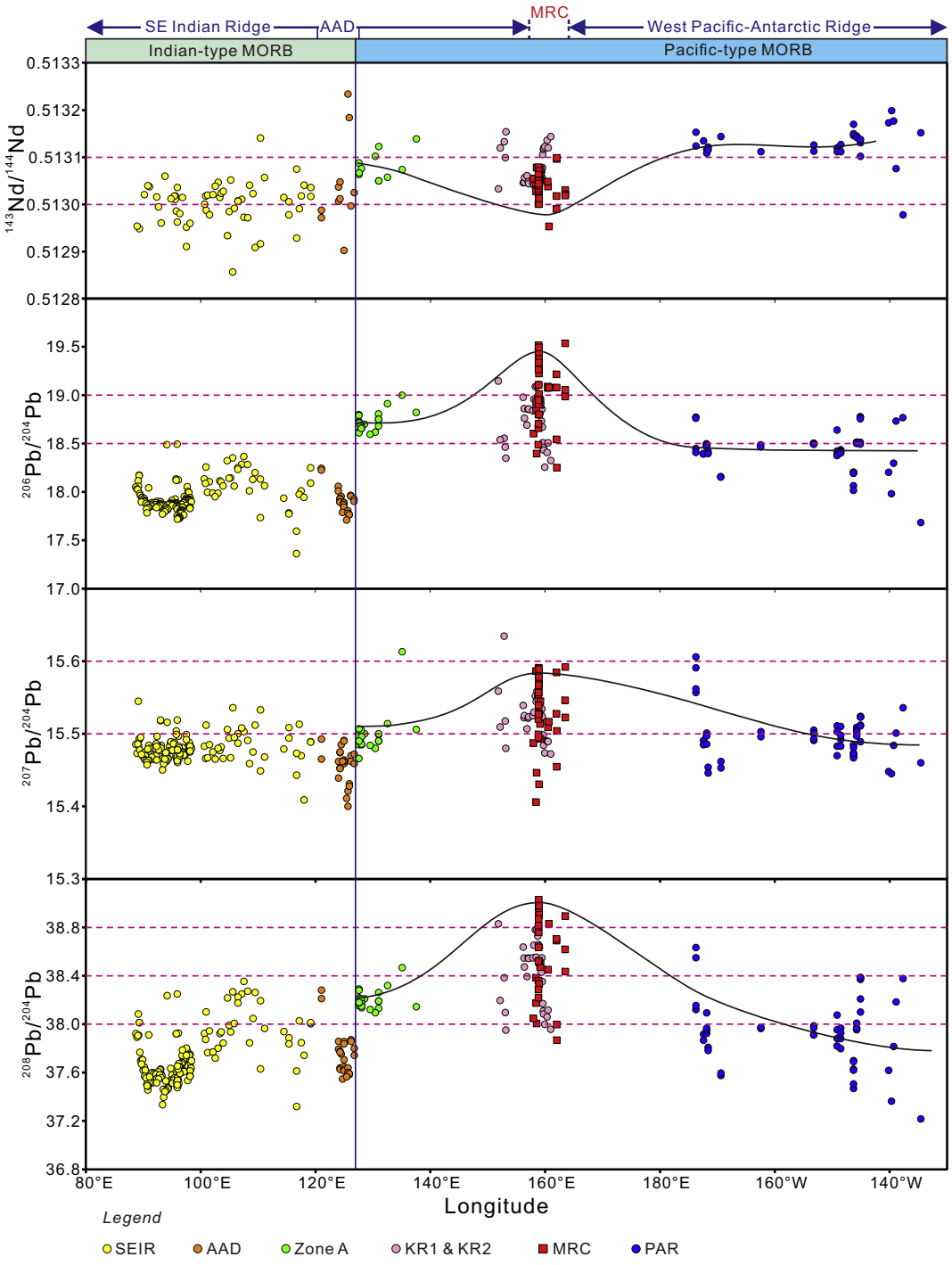

Fig. 10. Longitudinal variations of Pb and Nd isotopes for MORB from the western Pacific–Antarctic Ridge, Macquarie Ridge Complex and SE Indian Ridge. Data are available in Supplementary Table 4.

Symons, 2008). This is supported by the observation that metasomatism in the Zealandia peridotite xenoliths possess a large range of ages, with numerous ages <20 Ma despite the HIMU signature being added before 100 Ma (McCoy-West et al., 2016). Therefore, there is ongoing metasomatism in the Macquarie Basin oceanic lithosphere, probably as the result of remobilization of the Zealandia HIMU-like mantle components since the metasomatic event of the Zealandia lithospheric mantle at ~115–110 Ma (McCoy-West et al., 2016).

5.5. Possible links between MRC and other HIMU-like basalts in SW Pacific

Our new data support the hypothesis that the chemical characteristics of the MRC basalts were produced by melting of a heterogeneous mantle source, which consisted of a peridotitic asthenospheric mantle and pyroxenite veins. It is still unclear whether the distribution of the isotopically enriched component identified in the MRC rocks is restricted to the MRC and Zealandia areas, or if it occurs over a more

widespread portion of the mantle further west, east and south in the SW Pacific.

Indeed, for MORBs from further west and south in the Indian and Pacific Oceans (between the Australian–Antarctic discordance and the Udintsev Fracture Zone; Fig. 1a), relatively high Pb isotopic ratios and low Nd isotopic ratios similar to that of the MRC basalts have also been recorded from the Southeast Indian Ridge (SEIR) to the east of the Australian–Antarctic discordance, and two segments of the Pacific–Antarctic Ridge (Fig. 10; Park et al., 2019). This indicates that the HIMU component in the mantle source of the MRC basalts may extend both south and west beyond the MRC in the SW Pacific Oceans. We note that the HIMU-like isotope signature of the Pacific–Antarctic Ridge MORB was attributed to deep mantle upwelling related to the Balleny or Ross mantle plumes (Park et al., 2019). However, geochemical and isotopic evidence for the existence of deep mantle component in the mantle source of the Pacific–Antarctic Ridge MORB is lacking, and this model is not able to explain the generally higher Pb and lower Nd isotopic ratios of the MRC samples compared to the Pacific–Antarctic Ridge MORB (Fig. 10), which are closer to the Antarctic plumes (Figs. 1a, 9b).

Further south in Antarctica, HIMU-like basalts have been found in the Crary Mountains (Panter et al., 2000), Hobbs Coast (Hart et al., 1997) and the NW Ross Sea (Panter et al., 2018) in the West Antarctic Rift System (WARS), the Marie Byrd Seamounts (Kipf et al., 2014) and Ross Island (Phillips et al., 2018). Although the HIMU-like signatures of basalts from Hobbs Coast, Marie Byrd Seamounts and Ross Island were possibly derived from HIMU-type mantle plumes (Hart et al., 1997; Kipf et al., 2014; Phillips et al., 2018), the role of metasomatised Gondwana lithosphere has also been recognized (Panter et al., 2000; Panter et al., 2018). Metasomatic hydrous mineral phases have also been found in the Marie Byrd Land and Transantarctic mantle xenoliths (Gamble et al., 1988; Handler et al., 2003). We hypothesize that while some of these basalts could be derived from mantle plumes, at least portions of the west Antarctic lithospheric mantle were similarly affected by metasomatism from the subduction system that affected Zealandia, and thus contributed to the formation of the HIMU-like basalts across the region (Finn et al., 2005; McCoy-West et al., 2016; Panter et al., 2006).

On the periphery of the Antarctic lithosphere, the Scott Plateau and Balleny Plateau also have HIMU-like affinities and may also share this same pyroxenitic source. The Scott Plateau, in particular, shares geochemical and isotopic affinities with the MRC basalts (Figs. 5, 6, Supplementary Fig. 3). To explain the more isotopically radiogenic compositions of the Scott Plateau, a higher proportion of pyroxenite to peridotitic melt is required, which is consistent with the formation of highly alkaline rocks by low-degree partial melting under thick asthenospheric melts distal from the spreading centre (Fig. 1a, Fig. 9b). Conversely, the HIMU-like signatures of the Balleny province are different from those of the MRC (Fig. 7a–c). The generally higher $^{208}Pb/^{204}Pb$ and lower $^{143}Nd/^{144}Nd$ at given $^{206}Pb/^{204}Pb$ of the Balleny samples require higher time-integrated Th/Pb and lower time-integrated Sm/Nd source(s) compared with that of the MRC mantle source. Basalts from Balleny Plateau also have generally higher $^{143}Nd/^{144}Nd$ and lower Pb isotopic ratios than those of the south Tasman Seamounts (Fig. 1) but are similar to the Scott Plateau and MRC basalts (Figs. 5b, 6a–d). Assuming the Balleny province rocks are all from the same melting regime, the relatively recent magmatic products of the Balleny plume — the Balleny Plateau — may have entrained some pyroxenite melts, which could have caused the difference between the Balleny Plateau and the earlier south Tasman Seamounts, and similarities with the MRC and Scott Plateau (Fig. 9). Thus, the mechanisms that caused the heterogeneous isotopic signatures in the MRC and HIMU-like signatures in the Balleny Plateau and Scott Plateau may reflect a broader mantle anomaly rather than distinct plume-related signatures. The pyroxenitic component in the mantle source of the Balleny and Scott HIMU-like basalts could be derived from metasomatised oceanic lithospheric, or partial melts of the metasomatised Antarctic SCLM that were transported to the oceanic lithosphere by edge-driven convective mantle flow during the extension of the WARS (Fig. 9b; Panter et al., 2018).

6. Conclusions

New geochemical and Sr–Nd–Pb isotopic data from samples from the entire latitudinal length of the Macquarie Ridge Complex reveal similar N-MORB-like to E-MORB-like geochemical characteristics and isotopic ratios to that of Macquarie Island, which extend from depleted MORB towards a HIMU-like mantle component.

Mixing models using Monte Carlo simulations show that the isotopically enriched mantle component of the MRC basalts was not provided by the Balleny mantle plume, instead showing affinity with that of the HIMU-like basalts from Zealandia. Partial melting modelling indicates that the enriched component in the MRC basalts was produced by melting of small proportions of amphibole-bearing garnet pyroxenite in a dominantly peridotitic mantle. The correlations of partial melting proxies (e.g., $[La/Sm]_{CN}$) and Nd–Pb isotopic ratios indicate that low degree partial melts show higher proportions of isotopically enriched mantle signatures derived from the more fertile pyroxenitic component. The pyroxenite veins were likely generated in an oceanic lithospheric mantle affected by melts derived from delaminated metasomatised Zealandia SCLM, or affected by hydrous and carbonatitic fluids/melts derived from subducted material in the asthenosphere. The subducted material could be derived from ancient and/or recent subduction along the former Gondwana margin. This is consistent with the fact that the isotopically enriched mantle signature is found across the SW Pacific Ocean and adjacent continents affected by subduction along East Gondwana.

Declaration of Competing Interest

The authors declare that they have no known competing financial interests or personal relationships that could have appeared to influence the work reported in this paper.

Acknowledgements

This work was supported by the Australian Antarctic Division Science Project (grant number 4444). We thank the AAD staff at the Kensington headquarters and on Macquarie Island for support in managing the project, organizing the field trip and logistics. We are particularly thankful for support in the field from safety officer M. Raymond, ranger A. Turbett and station leader K. Williams. We are grateful to the Polar Rock Repository for providing four dredge samples for this study. QJ thanks for the support of the CSC–CIPRS scholarship. HB and RW were supported by the New Zealand Ministry of Business, Innovation and Employment (MBIE) Strategic Science Investment Fund, Marine Geological Processes and Resources (COPR1902). Comments from A. McCoy-West and V. Kamenetsky helped to improve an earlier version of this manuscript. We thank reviewers J. Mata and J. Geldmacher, and editor X.-H. Li for their helpful comments.

Appendix A. Supplementary data

Supplementary data to this article can be found online at https://doi.org/10.1016/j.lithos.2020.105893.

References

Adam, J., Green, T.H., Sie, S.H., 1993. Proton microprobe determined partitioning of Rb, Sr, Ba, Y, Zr, Nb and Ta between experimentally produced amphiboles and silicate melts with variable F content. Chem. Geol. 109 (1–4), 29–49.

Borghini, G., Rampone, E., Zanetti, A., Class, C., Fumagalli, P., Godard, M., 2020. Ligurian pyroxenite-peridotite sequences (Italy) and the role of melt-rock reaction in creating enriched-MORB mantle sources. Chem. Geol. 532.

Caroff, M., Bellon, H., Chauris, L., Carron, J.-P., Chevrier, S., Gardinier, A., Cotten, J., Moan, Y.L., Neidhart, Y., 1995. Magmatisme fissural triasico-liasique dans l'ouest du Massif Armoricain (France): pétrologie, géochimie, âge, et modalités de la mise en place. Can. J. Earth Sci. 32 (11), 1921–1936.

Chaffey, D., Cliff, R., Wilson, B., 1989. Characterization of the St Helena magma source. Geol. Soc. Lond. Spec. Publ. 42 (1), 257–276.

Conway, C.E., Bostock, H.C., Baker, J.A., Wysoczanski, R.J., Verdier, A.L., 2012. Evolution of Macquarie Ridge complex seamounts: Implications for volcanic and tectonic processes at the Australia-Pacific plate boundary south of New Zealand. Mar. Geol. 295, 34–50.

Coogan, L.A., MacLeod, C.J., Dick, H.J.B., Edwards, S.J., Kvassnes, A., Natland, J.H., Robinson, P.T., Thompson, G., O'Hara, M.J., 2001. Whole-rock geochemistry of gabbros from the Southwest Indian Ridge: constraints on geochemical fractionations between the upper and lower oceanic crust and magma chamber processes at (very) slow-spreading ridges. Chem. Geol. 178 (1–4), 1–22.

Dalpé, C., 1994. Partition coefficients for rare-earth elements between calcic amphibole and Ti-rich basanitic glass at 1.5 GPa, 1,100°C. Mineral. Mag. 58, 207–208.

Dijkstra, A.H., Sergeev, D.S., Spandler, C., Pettke, T., Meisel, T., Cawood, P.A., 2010. Highly refractory peridotites on Macquarie Island and the case for anciently depleted domains in the Earth's mantle. J. Petrol. 51 (1–2), 469–493.

Duncan, R.A., Varne, R., 1988. The age and distribution of the igneous rocks of Macquarie Island. Pap. Proc. R. Soc. Tasmania 122 (1), 45–50.

Finn, C.A., Müller, R.D., Panter, K.S., 2005. A Cenozoic diffuse alkaline magmatic province (DAMP) in the Southwest Pacific without rift or plume origin. Geochem. Geophys. Geosyst. 6.

Gamble, J., McGibbon, F., Kyle, P., Menzies, M., Kirsch, I., 1988. Metasomatised Xenoliths from Foster Crater, Antarctica: Implications for Lithospheric Structure and Processes beneath the Transantarctic Mountain Front. Journal of Petrology, pp. 109–138 Special Lithosphere Issue.

Goldstein, S.L., Soffer, G., Langmuir, C.H., Lehnert, K.A., Graham, D.W., Michael, P.J., 2008. Origin of a 'Southern Hemisphere' geochemical signature in the Arctic upper mantle. Nature 453 (7191), 89–93.

Haase, K.M., Goldschmidt, B., Garbe-Schönberg, C.-D., 2004. Petrogenesis of Tertiary continental intra-plate lavas from the Westerwald region, Germany. J. Petrol. 45 (5), 883–905.

Hamelin, B., Allègre, C.J., 1988. Lead isotope study of orogenic lherzolite massifs. Earth Planet. Sci. Lett. 91 (1–2), 117–131.

Handler, M.R., Wysoczanski, R.J., Gamble, J.A., 2003. Proterozoic lithosphere in Marie Byrd Land, West Antarctica: Re-Os systematics of spinel peridotite xenoliths. Chem. Geol. 196 (1–4), 131–145.

Hart, S.R., 1984. A large-scale isotope anomaly in the Southern Hemisphere mantle. Nature 309 (5971), 753–757.

Hart, S.R., 1988. Heterogeneous mantle domains: signatures, genesis and mixing chronologies. Earth Planet. Sci. Lett. 90 (3), 273–296.

Hart, S.R., Blusztajn, J., LeMasurier, W.E., Rex, D.C., 1997. Hobbs Coast Cenozoic volcanism: Implications for the West Antarctic rift system. Chem. Geol. 139 (1–4), 223–248.

Hirschmann, M.M., Stolper, E.M., 1996. A possible role for garnet pyroxenite in the origin of the "garnet signature" in MORB. Contrib. Mineral. Petrol. 124 (2), 185–208.

Hoernle, K., White, J.D.L., van den Bogaard, P., Hauff, F., Coombs, D.S., Werner, R., Timm, C., Garbe-Schonberg, D., Reay, A., Cooper, A.F., 2006. Cenozoic intraplate volcanism on New Zealand: Upwelling induced by lithospheric removal. Earth Planet. Sci. Lett. 248 (1–2), 350–367.

Hoernle, K., Hauff, F., van den Bogaard, P., Werner, R., Mortimer, N., Geldmacher, J., Garbe-Schonberg, D., Davy, B., 2010. Age and geochemistry of volcanic rocks from the Hikurangi and Manihiki oceanic Plateaus. Geochim. Cosmochim. Acta 74 (24), 7196–7219.

Hoernle, K., Timm, C., Hauff, F., Tappenden, V., Werner, R., Jolis, E., Mortimer, N., Weaver, S., Riefstahl, F., Gohl, K., 2020. Late cretaceous (99-69 Ma) basaltic intraplate volcanism on and around Zealandia: Tracing upper mantle geodynamics from Hikurangi Plateau collision to Gondwana breakup and beyond. Earth Planet. Sci. Lett. 529, 115864.

Hofmann, A.W., 1988. Chemical differentiation of the Earth: the relationship between mantle, continental crust, and oceanic crust. Earth Planet. Sci. Lett. 90 (3), 297–314.

Hofmann, A.W., 2003. Sampling mantle heterogeneity through oceanic basalts: Isotopes and trace elements. In: Carlson, R.W. (Ed.), Treatise on Geochemistry. Elsevier Science Ltd, Amsterdam, pp. 61–97.

Homrighausen, S., Hoernle, K., Hauff, F., Geldmacher, J., Wartho, J.-A., van den Bogaard, P., Garbe-Schönberg, D., 2018. Global distribution of the HIMU end member: Formation through Archean plume-lid tectonics. Earth Sci. Rev. 182, 85–101.

Husen, A., Kamenetsky, V.S., Everard, J.L., Kamenetsky, M.B., 2016. Transition from ultra-enriched to ultra-depleted primary MORB melts in a single volcanic suite (Macquarie Island, SW Pacific): Implications for mantle source, melting process and plumbing system. Geochim. Cosmochim. Acta 185, 112–128.

Ito, G., Mahoney, J.J., 2005. Flow and melting of a heterogeneous mantle: 1. Method and importance to the geochemistry of ocean island and mid-ocean ridge basalts. Earth Planet. Sci. Lett. 230 (1–2), 29–46.

Kamenetsky, V.S., Eggins, S.M., 2012. Systematics of metals, metalloids, and volatiles in MORB melts: Effects of partial melting, crystal fractionation and degassing (a case study of Macquarie Island glasses). Chem. Geol. 302, 76–86.

Kamenetsky, V.S., Maas, R., 2002. Mantle-melt evolution (dynamic source) in the origin of a single MORB suite: a perspective from magnesian glasses of Macquarie Island. J. Petrol. 43 (10), 1909–1922.

Kamenetsky, V.S., Everard, J.L., Crawford, A.J., Varne, R., Eggins, S.M., Lanyon, R., 2000. Enriched end-member of primitive MORB melts: petrology and geochemistry of glasses from Macquarie Island (SW Pacific). J. Petrol. 41 (3), 411–430.

Kamenetsky, V.S., Maas, R., Sushchevskaya, N.M., Norman, M.D., Cartwright, I., Peyve, A.A., 2001. Remnants of Gondwanan continental lithosphere in oceanic upper mantle: evidence from the South Atlantic Ridge. Geology 29 (3), 243–246.

Kendrick, M.A., Kamenetsky, V.S., Phillips, D., Honda, M., 2012. Halogen systematics (Cl, Br, I) in Mid-Ocean Ridge Basalts: a Macquarie Island case study. Geochim. Cosmochim. Acta 81, 82–93.

Kipf, A., Hauff, F., Werner, R., Gohl, K., van den Bogaard, P., Hoernle, K., Maicher, D., Klugel, A., 2014. Seamounts off the West Antarctic margin: a case for non-hotspot driven intraplate volcanism. Gondwana Res. 25 (4), 1660–1679.

Klein, E.M., Langmuir, C.H., 1987. Global correlations of ocean ridge basalt chemistry with axial depth and crustal thickness. J. Geophys. Res. Solid Earth 92 (B8), 8089–8115.

Lambart, S., Laporte, D., Schiano, P., 2009. An experimental study of pyroxenite partial melts at 1 and 1.5 GPa: Implications for the major-element composition of Mid-Ocean Ridge Basalts. Earth Planet. Sci. Lett. 288 (1–2), 335–347.

Lambart, S., Laporte, D., Provost, A., Schiano, P., 2012. Fate of pyroxenite-derived melts in the peridotitic mantle: Thermodynamic and experimental constraints. J. Petrol. 53 (3), 451–476.

Lambart, S., Koornneef, J.M., Millet, M.A., Davies, G.R., Cook, M., Lissenberg, C.J., 2019. Highly heterogeneous depleted mantle recorded in the lower oceanic crust. Nat. Geosci. 12 (6), 482–486.

Lanyon, R., 1994. Mantle Reservoirs and Mafic Magmatism Associated with the Break-up of Gondwana: the Balleny Plume and the Australian-Antarctic discordance: U-Pb Zircon Dating of a Proterozoic Mafic Dyke Swarm in the Vestfold Hills, East Antarctica. Ph.D. Thesis. University of Tasmania, Hobart.

Lanyon, R., Varne, R., Crawford, A.J., 1993. Tasmanian Tertiary basalts, the Balleny Plume, and opening of the Tasman Sea (Southwest Pacific Ocean). Geology 21 (6), 555–558.

Larter, R.D., Cunningham, A.P., Barker, P.F., Gohl, K., Nitsche, F.O., 2002. Tectonic evolution of the Pacific margin of Antarctica 1. Late Cretaceous tectonic reconstructions. J. Geophys. Res. Solid Earth 107 (B12) (EPM 5-1-EPM 5–19).

Laske, G., Masters, G., Ma, Z., Pasyanos, M., 2013. Update on CRUST1. 0—A 1-degree Global Model of Earth's CRUST. Geophysical Research Abstracts.

Le Bas, M.J., Le Maitre, R.W., Streckeisen, A., Zanettin, B., 1986. A chemical classification of volcanic rocks based on the total alkali-silica diagram. J. Petrol. 27 (3), 745–750.

Mahoney, J.J., Frei, R., Tejada, M.L.G., Mo, X.X., Leat, P.T., Nagler, T.F., 1998. Tracing the Indian Ocean mantle domain through time: Isotopic results from Old West Indian, East Tethyan, and South Pacific seafloor. J. Petrol. 39 (11—12), 1285–1306.

Massell, C., Coffin, M.F., Mann, P., Mosher, S., Frohlich, C., Duncan, C.S., Karner, G., Ramsay, D., Lebrun, J.F., 2000. Neotectonics of the Macquarie Ridge complex, Australia-Pacific plate boundary. J. Geophys. Res. Solid Earth 105 (B6), 13457–13480.

McCoy-West, A.J., Baker, J.A., Faure, K., Wysoczanski, R., 2010. Petrogenesis and origins of Mid-cretaceous continental intraplate volcanism in Marlborough, New Zealand: Implications for the long-lived HIMU magmatic mega-province of the SW Pacific. J. Petrol. 51 (10), 2003–2045.

McCoy-West, A.J., Bennett, V.C., Amelin, Y., 2016. Rapid Cenozoic ingrowth of isotopic signatures simulating "HIMU" in ancient lithospheric mantle: Distinguishing source from process. Geochim. Cosmochim. Acta 187, 79–101.

McKenzie, D., O'Nions, R.K., 1991. Partial melt distributions from inversion of rare-earth element concentrations. J. Petrol. 32 (5), 1021–1091.

Meckel, T.A., 2003. Tectonics of the Hjort Region of the Macquarie Ridge Complex, Southernmost Australian-Pacific Plate Boundary, Southwest Pacific Ocean. Ph.D. Thesis. The University of Texas at Austin, Austin, Texas.

Merle, R., Marzoli, A., Aka, F.T., Chiaradia, J., Reisberg, L., Castorina, F., Jourdan, F., Renne, P., N'ni, J., Nyobe, J., 2017. Mt Bambouto Volcano, Cameroon Line: mantle source and differentiation of within-plate alkaline rocks. J. Petrol. 58 (5), 933–962.

Morgan, J.P., 1999. Isotope topology of individual hotspot basalt arrays: Mixing curves or melt extraction trajectories? Geochem. Geophys. Geosyst. 1.

Mosher, S., Symons, C.M., 2008. Ridge reorientation mechanisms: Macquarie ridge complex, Australia-Pacific plate boundary. Geology 36 (2), 119–122.

Niu, Y.L., 1997. Mantle melting and melt extraction processes beneath ocean ridges: evidence from abyssal peridotites. J. Petrol. 38 (8), 1047–1074.

Niu, Y.L., O'Hara, M.J., 2003. Origin of ocean island basalts: a new perspective from petrology, geochemistry, and mineral physics considerations. J. Geophys. Res. Solid Earth 108 (B4).

O'Hara, M., Richardson, S., Wilson, G., 1971. Garnet-peridotite stability and occurrence in crust and mantle. Contrib. Mineral. Petrol. 32 (1), 48–68.

Panter, K.S., Hart, S.R., Kyle, P., Blusztanjn, J., Wilch, T., 2000. Geochemistry of late Cenozoic basalts from the Crary Mountains: characterization of mantle sources in Marie Byrd Land, Antarctica. Chem. Geol. 165 (3–4), 215–241.

Panter, K.S., Blusztajn, J., Hart, S.R., Kyle, P.R., Esser, R., McIntosh, W.C., 2006. The origin of HIMU in the SW Pacific: evidence from intraplate volcanism in southern New Zealand and subantarctic islands. J. Petrol. 47 (9), 1673–1704.

Panter, K.S., Castillo, P., Krans, S., Deering, C., McIntosh, W., Valley, J.W., Kitajima, K., Kyle, P., Hart, S., Blusztajn, J., 2018. Melt origin across a rifted continental margin: a case for subduction-related metasomatic agents in the lithospheric source of alkaline basalt, NW Ross Sea, Antarctica. J. Petrol. 59 (3), 517–557.

Park, S.H., Langmuir, C.H., Sims, K.W.W., Blichert-Toft, J., Kim, S.S., Scott, S.R., Lin, J., Choi, H., Yang, Y.S., Michael, P.J., 2019. An isotopically distinct Zealandia-Antarctic mantle domain in the Southern Ocean. Nat. Geosci. 12 (3), 206–214.

Peate, D.W., Breddam, K., Baker, J.A., Kurz, M.D., Barker, A.K., Prestvik, T., Grassineau, N., Skovgaard, A.C., 2010. Compositional characteristics and spatial distribution of enriched Icelandic mantle components. J. Petrol. 51 (7), 1447–1475.

Phillips, E.H., Sims, K.W.W., Blichert-Toft, J., Aster, R.C., Gaetani, G.A., Kyle, P.R., Wallace, P.J., Rasmussen, D.J., 2018. The nature and evolution of mantle upwelling at Ross Island, Antarctica, with implications for the source of HIMU lavas. Earth Planet. Sci. Lett. 498, 38–53.

Pyle, D., Christie, D.M., Mahoney, J., Duncan, R.A., 1995. Geochemistry and geochronology of ancient southeast Indian and Southwest Pacific seafloor. J. Geophys. Res. Solid Earth 100 (B11), 22261–22282.
Rehkämper, M., Hofmann, A.W., 1997. Recycled Ocean crust and sediment in Indian Ocean MORB. Earth Planet. Sci. Lett. 147 (1–4), 93–106.
Saunders, A.D., Norry, M.J., Tarney, J., 1988. Origin of MORB and chemically-depleted mantle reservoirs: Trace element constraints. J. Petrol. (1), 415–445 Special Volume.
Schilling, J.G., Hanan, B.B., Mccully, B., Kingsley, R.H., Fontignie, D., 1994. Influence of the Sierra Leone mantle plume on the equatorial Mid-Atlantic Ridge: a Nd-Sr-Pb isotopic study. J. Geophys. Res. Solid Earth 99 (B6), 12005–12028.
Scott, J.M., Brenna, M., Crase, J.A., Waight, T.E., van der Meer, Q.H.A., Cooper, A.F., Palin, J.M., Le Roux, P., Munker, C., 2016. Peridotitic lithosphere metasomatized by volatile-bearing melts, and its association with intraplate alkaline HIMU-like magmatism. J. Petrol. 57 (10), 2053–2078.
Shaw, D.M., 1970. Trace element fractionation during anatexis. Geochim. Cosmochim. Acta 34 (2), 237–243.
Stracke, A., Hofmann, A.W., Hart, S.R., 2005. FOZO, HIMU, and the rest of the mantle zoo. Geochem. Geophys. Geosyst. 6.
Sun, S.-S., McDonough, W.F., 1989. Chemical and isotopic systematics of oceanic basalts: implications for mantle composition and processes. Geol. Soc. Lond. Spec. Publ. 42 (1), 313–345.
Thirlwall, M.F., Upton, B.G.J., Jenkins, C., 1994. Interaction between continental lithosphere and the Iceland plume—Sr-Nd-Pb isotope geochemistry of Tertiary basalts, NE Greenland. J. Petrol. 35 (3), 839–879.
Tiepolo, M., Oberti, R., Zanetti, A., Vannucci, R., Foley, S.F., 2007. Trace-element partitioning between amphibole and silicate melt. Rev. Mineral. Geochem. 67, 417–451.
Timm, C., Hoernle, K., Werner, R., Hauff, F., van den Bogaard, P., White, J., Mortimer, N., Garbe-Schonberg, D., 2010. Temporal and geochemical evolution of the Cenozoic intraplate volcanism of Zealandia. Earth Sci. Rev. 98 (1–2), 38–64.
Van der Meer, Q., Waight, T.E., Scott, J., Münker, C., 2017. Variable sources for cretaceous to recent HIMU and HIMU-like intraplate magmatism in New Zealand. Earth Planet. Sci. Lett. 469, 27–41.
Van Orman, J.A., Grove, T.L., Shimizu, N., 2001. Rare earth element diffusion in diopside: influence of temperature, pressure, and ionic radius, and an elastic model for diffusion in silicates. Contrib. Mineral. Petrol. 141 (6), 687–703.
Varne, R., Brown, A.V., Falloon, T., 2000. Macquarie Island: its geology, structural history, and the timing and tectonic setting of its N-MORB to E-MORB magmatism. Geol. Soc. Am. Spec. Pap. 301–320.
Walter, M.J., 1998. Melting of garnet peridotite and the origin of komatiite and depleted lithosphere. J. Petrol. 39 (1), 29–60.
Wang, K., Plank, T., Walker, J.D., Smith, E.I., 2002. A mantle melting profile across the Basin and Range, SW USA. J. Geophys. Res. Solid Earth 107 (B1) (ECV 5-1-ECV 5-21).
Waters, C.L., Sims, K.W.W., Perfit, M.R., Blichert-Toft, J., Blusztajn, J., 2011. Perspective on the genesis of E-MORB from chemical and isotopic heterogeneity at 9–10°N East Pacific rise. J. Petrol. 52 (3), 565–602.
Wertz, K.L., 2003. From Seafloor Spreading to Uplift: the Structural and Geochemical Evolution of Macquarie Island on the Australian-Pacific Plate Boundary. Ph.D. Thesis. The University of Texas at Austin, Austin, Texas.
Yaxley, G.M., Kamenetsky, V., 1999. In situ origin for glass in mantle xenoliths from southeastern Australia: insights from trace element compositions of glasses and metasomatic phases. Earth Planet. Sci. Lett. 172 (1–2), 97–109.
Yaxley, G.M., Crawford, A.J., Green, D.H., 1991. Evidence for carbonatite metasomatism in spinel peridotite xenoliths from western Victoria, Australia. Earth Planet. Sci. Lett. 107 (2), 305–317.